nature cell biology

Proof-by-synthesis of the transcriptional logic of mammalian circadian clocks

Maki Ukai-Tadenuma[1,3], Takeya Kasukawa[2,3] and Hiroki R. Ueda[1,2,4]

Mammalian circadian clocks consist of complex regulatory loops mediated through—at least—morning, daytime and night-time DNA elements. To prove the transcriptional logic of mammalian clocks, we developed an *in cellulo* mammalian cell-culture system that allowed us to design and implement artificial transcriptional circuits. Here we show that morning activation and night-time repression can yield the transcriptional output during the daytime, and similarly that daytime activation and morning repression can yield night-time transcriptional output. We also observed that the diverse transcriptional outputs of other phases can be generated through the expression of simple combinations of transcriptional activators and repressors. These results reveal design principles not only for understanding the continuous transcriptional outputs observed *in vivo* but also for the logical construction of artificial promoters working at novel phases. Logical synthesis of artificial circuits, with an identified structure and observed dynamics, provides an alternative strategy applicable to the investigation of complex biological systems.

The transcriptional circuit underlying mammalian circadian clocks consists of at least three clock-controlled DNA elements (CCEs): morning (E-box/E´-box, CACGT[G/T])[1–4], daytime (D-box, TTA[T/C]GTAA)[4,5] and night-time (RRE, [A/T]A[A/T]NT[A/G]GGTCA)[6–8], and at least 20 clock or clock-controlled genes[4,7,9–28] (Fig. 1a). E-box-mediated transcription is directly or indirectly controlled by at least 11 transcription factors[9–21] and thus has a critical function as the core of mammalian circadian clocks[4,29], whereas the D-box-mediated and RRE-mediated transcriptions are controlled by four[9,24–26] and five[4,7,9,27,28] transcription factors, respectively, and function primarily as output or stabilizing loops[4,7,9,25–27] of mammalian circadian clocks.

Although the network structure of these *cis*-elements and *trans*-regulators has been described comprehensively[4], the dynamic principles governing this transcriptional circuit remain elusive. With an eye towards gaining a system-level understanding of the transcriptional logic underlying mammalian circadian clocks, we carefully reviewed its network structure (Fig. 1a). First, we examined the daytime expression mediated through the D-box, which is bound competitively by its transcriptional activators (*Dbp*, *Tef* and *Hlf*) and its transcriptional repressor (*E4bp4*). *Dbp*, *Tef* and *Hlf* are expressed during the morning under the control of the E-box, whereas *E4bp4* is expressed during the night-time under the control of the RRE[4]. On the basis of this circuit information, we formed the hypothesis that one (or more) morning activator(s) and a night-time repressor could together determine the daytime transcriptional output mediated through the D-box. Similarly, we examined the night-time expression mediated through the RRE, which is bound competitively by its activators (*Rorα*, *Rorβ* and *Rorγ*) and its repressors (*RevErbAα* and *RevErbAβ*). Because two of the three RRE activators (*Rorα* and *Rorβ*) are expressed during the daytime under the control of the D-box, and because the RRE repressors (*RevErbAα* and *RevErbAβ*) seem strongly influenced by the two morning elements (E-boxes) in their intronic promoter regions for their morning expression, we formulated another simple hypothesis: one or more daytime activators and one or more morning repressors can specify the night-time transcriptional output by regulating the RRE. As an initial investigation into the dynamic principles governing circadian transcriptional circuits, we focused on the daytime and night-time expression among three timings in mammalian circadian clocks. To test the hypotheses derived above (from examining the natural circadian circuit) we synthesized artificial transcriptional circuits to simulate the natural circuits physically and then observed the resulting system dynamics.

RESULTS

In cellulo mammalian cell-culture system for physical simulation of natural transcriptional circuits

We developed an *in cellulo* mammalian cell-culture system consisting of mouse clock cells (NIH3T3 (ref. 30)), an artificial activator (destabilized GAL4–VP16 fusion proteins, dGAL4–VP16), an artificial repressor (destabilized GAL4 proteins, dGAL4), and an output reporter harbouring a gene encoding destabilized luciferase (*dLuc*) driven by a minimal cytomegalovirus promoter (CMVmini) fused with

[1]Laboratory for Systems Biology, and [2]Functional Genomics Unit, Center for Developmental Biology, RIKEN, 2-2-3 Minatojima-minamimachi, Chuo-ku, Kobe, Hyogo, 650-0047, Japan.
[3]These authors contributed equally to this work.
[4]Correspondence and requests for materials should be addressed to H.R.U. (e-mail: uedah-tky@umin.ac.jp).

Received 16 June 2008; accepted 8 August 2008; published online 21 September 2008; DOI: 10.1038/ncb1775

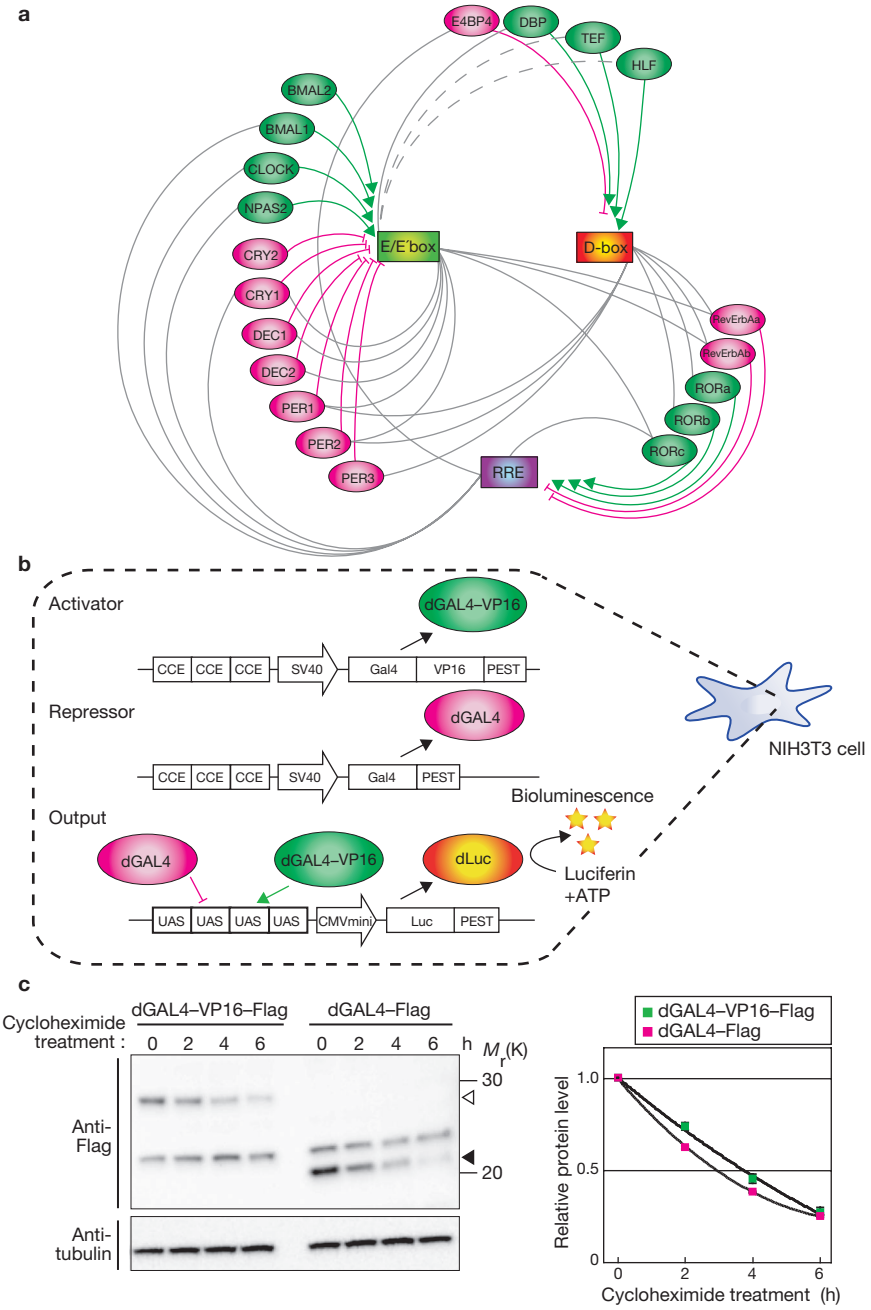

Figure 1 Using an *in cellulo* mammalian cell-culture system for the physical simulation of natural transcriptional circuits. (**a**) The natural transcriptional circuit of mammalian circadian clocks. Clock-controlled elements (CCE; rectangles), transcriptional activators (green ovals) and repressors (magenta ovals) are indicated. Grey lines between CCEs and transcription factors (that is, activators or repressors) indicate that the evolutionarily conserved CCEs are located on the promoter (or enhancer) regions of the respective transcription factor genes (grey dotted lines indicate putative CCEs determined by bioinformatics analysis). Green lines from transcriptional activators to CCEs indicate activation; magenta lines from transcriptional repressors to CCEs indicate repression. (**b**) The artificial transcriptional system synthesized in this study. A destabilized (that is, PEST-fused) GAL4–VP16 fusion protein (dGAL4–VP16) and destabilized GAL4 protein (dGAL4) were used as the activator and repressor, respectively (top and middle). These transcription factors are expressed under the control of three tandem repeats of clock-controlled (DNA) elements (CCEs). Once expressed, the artificial activator and repressor competitively bind the four tandem repeats of the galactose UAS in the artificial promoter to regulate the output reporter gene, encoding destabilized luciferase (*dLuc*, bottom). SV40, SV40 promoter; CMVmini, minimal CMV promoter. (**c**) Western blot analysis by cycloheximide treatment experiments revealed the protein half-life of dGAL4–VP16–Flag or dGAL4–Flag. The levels of dGAL4–VP16–Flag (white arrowhead) and dGAL4–Flag (black arrowhead) proteins were normalized by using tubulin-α protein levels as a loading control (left panel). Quantitative densitometric analysis shows the comparable half-lives of dGAL4–VP16–Flag and dGAL4–Flag to be 3.76 h and 2.96 h, respectively (right panel). The protein levels are shown relative to $t = 0$.

four tandem repeats of the galactose upstream activating sequence (UAS; Supplementary Text and Supplementary Fig. S1a), which are bound by the GAL4 DNA-binding domain (Fig. 1b). This system is designed on the basis of a previous finding[31] that the hybrid protein GAL4–VP16 can activate transcription efficiently in mammalian cells but the GAL4 protein alone cannot. We found that the half-lives of

dGAL4–VP16 and dGAL4 were comparable in our system: 3.76 h and 2.96 h, respectively (Fig. 1c). Thus, by extension, the artificial activator and repressor can competitively regulate the output reporter through the UAS. Finally, the artificial activator and repressor are driven by the SV40 basic promoter fused with three tandem repeats of CCEs (Supplementary Text and Supplementary Fig. S1b). We control the expression of these artificial regulators by using either the morning (E´-box), the daytime (D-box) or the night-time (RRE) elements as the CCEs[4]. To observe the dynamic behaviour of this artificial circuit, NIH3T3 host cells were transiently transfected with activator, repressor and reporter plasmids, stimulated with forskolin to synchronize the circadian rhythmicity of the individual cellular clocks, and then monitored in real time for bioluminescence over several days.

We reasoned that if (and only if) the peak timing of the expression (that is, the 'phase') of the transcriptional activator(s) and repressor(s) is a good determinant of the phase of the downstream transcriptional output, it should be possible to generate the natural phases in the clock cells by using synthetic transcription factors and promoters. If so, the finding would be remarkable because transcription factors are regulated by various post-transcriptional mechanisms[32], including translation[33], phosphorylation[9,22,34–38], ubiquitylation[9,38–40], sumoylation[41] and nuclear transportation[9,40,42]—these post-transcriptional mechanisms are thought to contribute, at least in part, to the phases of the downstream transcriptional outputs. In other words, a successful reconstruction of the natural circadian phases would imply that the network structure of transcriptional circuits determines the fundamental timing of the outputs from the circadian system. After transcription, the system output timing can then be reinforced or modified by the various post-transcriptional mechanisms listed above.

Proof-by-synthesis of daytime and night-time transcriptional regulations

Using the artificial circuit system (Fig. 1b), we attempted to test our hypothesis for daytime output by examining the dynamic behaviour of the transcriptional output generated by an artificial morning activator and an artificial night-time repressor, which were controlled by E´-box elements and RRE elements, respectively. We first confirmed the circadian oscillations of output *dLuc* messenger RNA (mRNA), as well as the timing of the binding of the activator (dGAL4–VP16) and repressor (dGAL4) to the UAS—the peak times were at 2.0 h, 3.0 h and 16.0 h before the second peak of output luciferase activity, respectively (Fig. 2a, b, and Supplementary Fig. S1c). We noted that the peak time of output mRNA abundance closely (within about 1.0 h) matched the peak time of the activator binding in our *in cellulo* system. Natural circadian systems show similar timing between the peak times of mRNA output and activator binding to the DNA element—at least for E-box activators (BMAL1/CLOCK)—where the peak time of E-box-controlled mRNA expression is at zeitgeber time (ZT) 7 (ref. 43) which is in the middle of the range of peak time binding of BMAL1/CLOCK to the E-box, ZT 6–8.

When monitored by luciferase activity, the phases of the activator and repressor in this experiment were detected at circadian time (CT) 4.0 ± 0.29 (s.d., $n = 3$), and CT 17.1 ± 0.37 ($n = 3$; Fig. 2c and Supplementary Fig. S2a, left). The transcriptional output driven by these regulators showed circadian oscillation with a phase at CT 7.7 ± 0.85 ($n = 4$), which is close (1.0 h or less) to the corresponding natural daytime (D-box) phase, CT 8.7 ± 1.13. This result suggests that morning activation and night-time repression are sufficient to determine the daytime transcriptional output. High-amplitude circadian oscillation was not detected by expressing either the morning activator or the night-time repressor alone (Supplementary Fig. S2b). Even when we used the thymidine kinase (TK) promoter fused with 3 × CCE as a weaker driver, which generates sevenfold less expression than the SV40 promoter (1:(7.28 ± 0.70); Supplementary Fig. S2b, left), we still could not detect high-amplitude circadian oscillations (Supplementary Fig. S2b). These results illustrate that the competition between a morning activator and night-time repressor is essential for generating detectable circadian oscillations during daytime, which confirms observations of natural circadian systems, in which a morning activator (*Dbp*, *Tef* or *Hlf*) and a night-time repressor (*E4bp4*) also competitively bind to the D-box element[9,24–26]. Through this competitive binding, we speculate that the D-box element can integrate both the morning-phase information conferred by its activator (*Dbp*, *Tef* or *Hlf*) and the night-time-phase information conferred by its repressor (*E4bp4*) to generate the daytime information.

We next tested the hypothesis for night-time output by examining another artificial circuit, consisting of an artificial daytime activator under D-box control and a morning repressor under E´-box control (Fig. 2d and Supplementary Fig. S2a, right). When monitored by luciferase activity, the phases of a transcriptional activator and repressor in this experiment were at CT 8.7 and 9.1 (mean = 8.9, $n = 2$) and CT 3.8 and 4.0 (mean = 3.9, $n = 2$), respectively. The transcriptional output driven by the regulators showed circadian oscillation with its phase at CT 16.6 ± 1.04 ($n = 3$), which is also very close (1.0 h or less) to the corresponding natural night-time phase (CT 17.0 ± 0.81). As with the daytime transcriptional output, a high-amplitude circadian oscillation could not be generated by expressing the daytime activator or morning repressor alone (Supplementary Fig. S2b). These results therefore also confirmed that the competition between a daytime activator and a morning repressor is important in generating detectable circadian oscillation during the night-time in cells. Together, our reconstruction experiments for daytime and night-time expressions imply that the input phases of transcription factors can determine the phases of transcriptional output.

Synthesis of novel output phases *in cellulo* and *in vivo*

These findings led us to reason that various combinations of transcription factors with CCEs for the three basic circadian phases (morning, daytime and night-time) might generate not only the basic phases, such as daytime and night-time, but also other phases. To explore this possibility, we examined artificial circuits with various other activator–repressor pairs. In a circuit with an artificial night-time activator under RRE control and a daytime repressor under D-box control, we observed high-amplitude circadian output with the phase at CT 22.2 ± 0.70 ($n = 4$), which is 1.8 h before a subjective dawn (Fig. 3a and Supplementary Fig. S2c, left). We then tested the remaining combinations of regulators: that is, a night-time activator and a morning repressor, a morning activator and a daytime repressor, and a daytime activator and a night-time repressor. All of these artificial circuits showed circadian transcriptional outputs, with phases at CT 20.6 ± 0.91 (s.d, $n = 4$; a subjective late night), CT 4.7 ± 0.40 (s.d., $n = 3$; 1.3 h before a subjective noon) and CT 11.0 ± 0.79 (s.d., $n = 3$; 1.0 h before a subjective dusk), respectively (Fig. 3b–d and Supplementary Fig. S2c). From these results we concluded that, through simple combinations of the transcription factors of the three basic circadian phases, we can generate diverse transcriptional outputs that peak close to a subjective noon, dawn, dusk or late night.

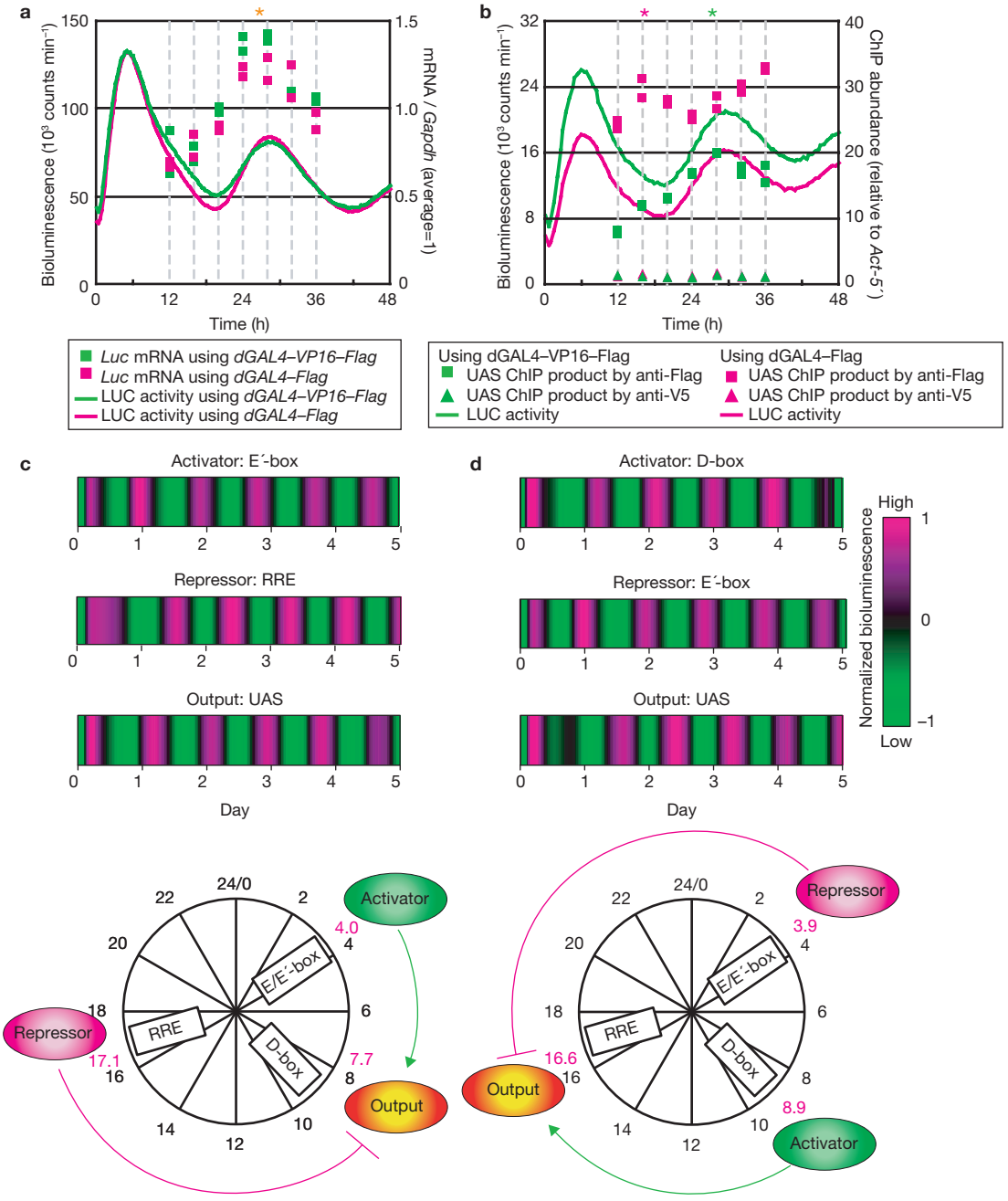

Figure 2 Proof-by-synthesis of daytime and night-time transcriptional regulations. (**a**) Quantification of the output *dLuc* mRNA from the artificial output reporter. The amounts of *dLuc* mRNA relative to constitutively expressed *Gapdh* (glyceraldehyde-3-phosphate dehydrogenase) mRNA (points) are indicated along with the luciferase (LUC) activity (lines) for two different artificial transcriptional circuits: one using *dGAL4–VP16–Flag* (green) and another using *dGal4–Flag* (magenta). The estimated peak of output *dLuc* mRNA (marked with an orange asterisk) occurs 2.0 h before the second peak of output luciferase activity. (**b**) Quantification of GAL4–VP16–Flag and GAL4–Flag bindings to the UAS in artificial transcriptional circuits. After normalization for the amount of input DNA, the amounts of UAS regions immunoprecipitated by anti-Flag antibody (squares) and by anti-V5 antibody (triangles) were quantified relative to a constitutively unbound *actin* promoter region (*Act-5′*). These relative amounts of UAS ChIP products are indicated along with the luciferase activity (line) for two different artificial transcriptional circuits using dGAL4–VP16–Flag (green) and dGAL4–Flag (magenta) (see also Supplementary Fig. S1c for other results of the negative control). The estimated peak times of UAS ChIP products bound by the activator (dGAL4–VP16, marked with a green asterisk) and the repressor (dGAL4, marked with a magenta asterisk) were 3.0 and 16.0 h before the second peak of output luciferase activity, respectively. (**c**, **d**) Synthesis of daytime or night-time expressions from two different artificial transcriptional circuits: morning activator under E′-box control and night-time repressor under RRE control (**c**), and daytime activator under D-box control and morning repressor under E′-box control (**d**). Heat maps (top) indicate high (magenta) or low (green) representative promoter activities and output of each artificial transcriptional circuit monitored by bioluminescence from NIH3T3 cells. The bioluminescence data were detrended in baseline and amplitude, then normalized to set their maximum, minimum and average to 1, –1 and 0, respectively (see also Supplementary Fig. S2a for the raw bioluminescence data). The schemes at the bottom summarize the timings of peaks (that is, 'phases') of promoter activity, where an activator (green oval), repressor (magenta oval) and output reporter (orange oval) are indicated with their phases in circadian time (magenta numbers).

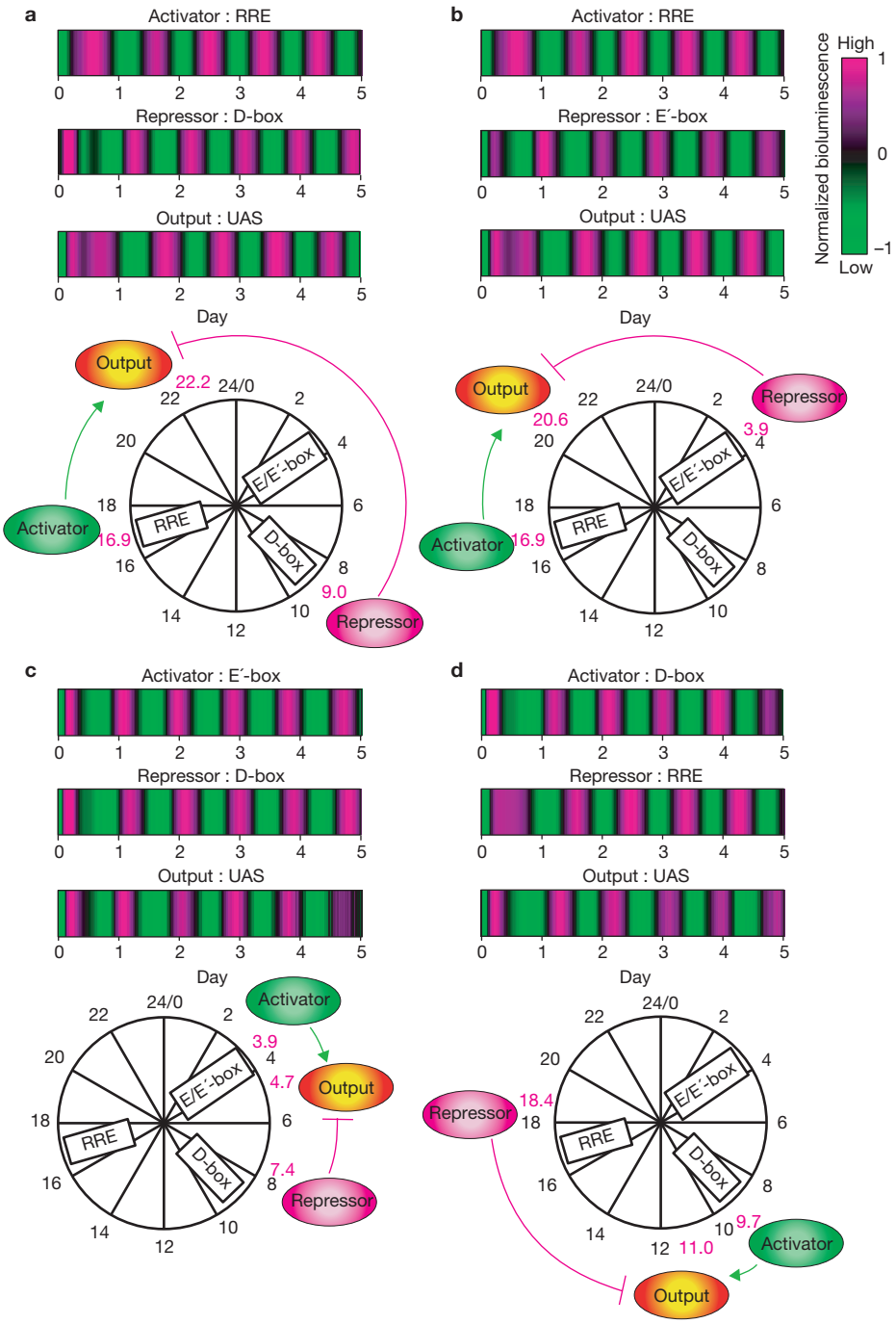

Figure 3 Synthesis of various output phases from three basic circadian phases in artificial transcriptional circuits. Promoter activities of an activator, repressor and output reporter in four different artificial transcriptional circuits: (**a**) night-time activator under RRE control and daytime repressor under D-box control, (**b**) night-time activator under RRE control and morning repressor under E′-box control, (**c**) morning activator under E′-box control and daytime repressor under D-box control, and (**d**) daytime activator under D-box control and night-time repressor under RRE control. Heat maps at the top indicate representative promoter activities, and the schemes at the bottom summarize the results, as described for Fig. 2 (see also Supplementary Fig. S2c for the raw bioluminescence data).

Even if the phase of the activator was not changed, an advance or delay in the repressor phase led to a corresponding change in the phase of transcriptional output (Fig. 4a–c). Conversely, a change in the activator phase also led to a corresponding alteration in the output phase (Supplementary Fig. S3). We can deduce from these findings that mammalian circadian clocks can start from three basic circadian phases to generate finally, through the transcriptional cascade, practically continuous phases, which have been observed *in vivo* in central and peripheral clock tissues including the suprachiasmatic nucleus, heart and liver[8,44–46]. This concept is reinforced by our observations that many transcription factors are expressed rhythmically at various phases in the liver (Fig. 4d), and that some seem to be controlled directly by the circadian clock through

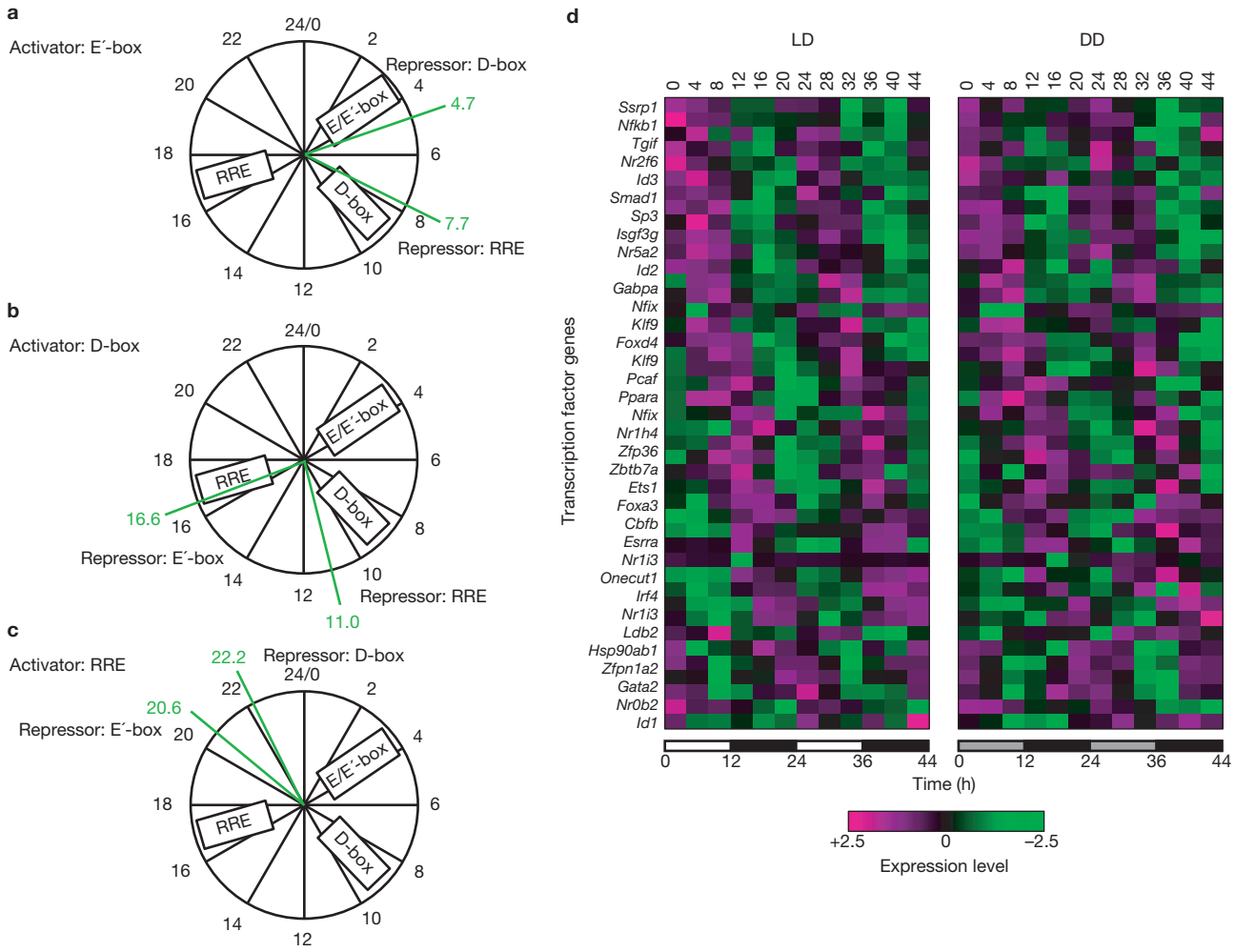

Figure 4 Transcriptional mechanisms to generate various output phases. (**a**–**c**) Output phases in artificial transcriptional circuits with a morning activator (**a**), daytime activator (**b**) or night-time activator (**c**). The phase of an output reporter (green lines and numbers) is indicated in circadian time (hours) for each repressor used. In artificial transcriptional circuits *in cellulo*, the output phase could be changed according to the input phase of the repressor even if that of the activator was unchanged. (**d**) *In vivo* periodic gene expression of various known transcription factors in mouse liver under light/dark (LD) and constant darkness (DD) conditions. Columns represent time points, and rows represent the probe sets for transcription factors. The expression levels of each probe set were normalized so that their average and standard deviation were set to 0 and 1, respectively.

E-boxes, D-boxes or RREs (Supplementary Table S1). Furthermore, transcriptional activator(s) and repressor(s) binding to similar DNA elements are expressed at various phases *in vivo* (Supplementary Table S1), and are therefore expected, from our *in cellulo* findings, to generate additional output phases.

Transcriptional logic underlying mammalian circadian clocks

On the basis of the findings in this study, we can now examine two predictions on the timing ('phase') and relative amplitude of circadian output oscillations in our previous report[4], which proposed that the phase advancement of a repressor relative to an activator causes a phase delay of expression ('repressor-precedes-activator' mechanism), whereas the phase advancement of an activator relative to a repressor causes a phase advancement of expression ('activator-precedes-repressor' mechanism). The previous paper also proposed that a larger phase difference between an activator and a repressor generates a greater relative amplitude of output rhythm ('repressor-antiphasic-to-activator' mechanism). To verify these predictions, we modelled the transcriptional system by using an activator, a repressor and an output reporter. To implement this transcriptional system numerically, we searched for the sets of parameters that could reproduce the observed reporter output of the *in cellulo* mammalian cell-culture system (see Supplementary Text). We then plotted the theoretical relationship between the output phases (the delay/advancement of output expressions) and the input phases (the phase differences between activators and repressors; Fig. 5a) and found that the experimental data (coloured dots) matched the theoretical plot (black line). This supported the 'repressor-precedes-activator' and 'activator-precedes-repressor' mechanisms for the output phases. These repressor-precedes-activator and activator-precedes-repressor mechanisms can delay or advance the default output phase (Fig. 5a, dashed line) to generate new output phases, respectively (see also Fig. 5a, green circle and square), which probably serve to create the seemingly continuous output phases observed *in vivo*[8,44–46].

We also plotted the theoretical relationship between the relative amplitudes of outputs and the input phases (the phase differences between activators and repressors; Fig. 5b). We noticed that some outliers had

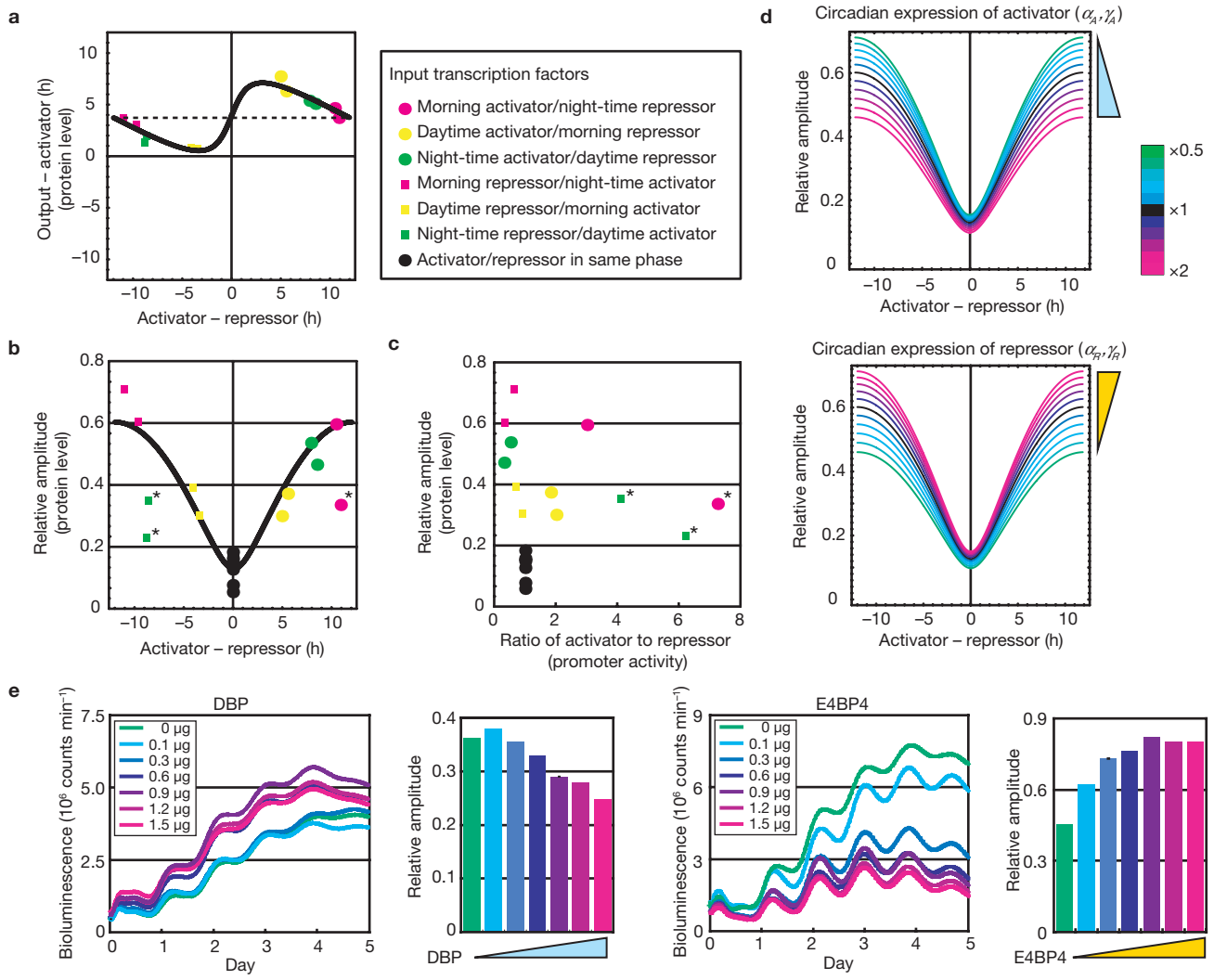

Figure 5 Transcriptional logic underlying mammalian circadian clocks. (**a**) Observed and simulated relationships between input transcription factors and the phase of the output reporter. Axes represent the phase differences (hours) between activator and repressor (*x* axis) and between output and activator (*y* axis). Points show the means of the measurement data (duplicated independently)—different point colour and shape combinations represent different transcription factor combinations. The curve shows a simulated relationship calculated from a theoretical model. The dashed line (at about +4 h) shows the default output reporter phase that occurs when a repressor is antiphasic to an activator. (**b**) Observed and simulated relationships between input transcription factors and the relative amplitude of the output reporter. The *y* axis represents the relative amplitude of the output reporter. The curve shows a simulated relationship calculated from our theoretical model. The points marked with an asterisk indicate outliers that have a lower relative amplitude (by 0.2 or more) than the predicted curve. (**c**) Observed relationships between the changes in expression levels of input transcription factors and the relative amplitude of the output reporter. The *x* axis represents the ratio of activator expression to repressor expression. The outlier points marked with an asterisk indicate experiments in which there was a large difference (more than fourfold) in the expression levels of activator relative to repressor (the points marked with an asterisk here are consistent with the outliers from **b**). (**d**) The predicted sensitivity of the relative amplitude when the circadian expression of an activator or a repressor is changed fourfold (proportional changes in the expression level of transcription factor affect both amplitude α and baseline γ simultaneously). Activator or repressor expression levels were varied fourfold (from ×0.5 to ×2); the coloured curves indicate the predicted effects of these changes in expression levels of transcription factors on relative amplitude of reporter output. (**e**) Perturbation experiments of natural transcriptional circuits. The relative amplitudes of luciferase activity are derived from the raw bioluminescence data of a daytime output reporter (p3 × D-box-SV40-*dLuc*) for various amounts of activator (DBP from p3 × E′-box-SV40-*Dbp*) or repressor (E4BP4 from p3 × RRE-SV40-*E4bp4*). Shown are the averages of the raw bioluminescence data from two or three independent samples.

a lower relative amplitude (by 0.2 or more; Fig. 5b, asterisked) than the predicted curve (Fig. 5b, black line), which seems to have been due to the larger changes (fourfold or more) in the expression levels of activator or repressor (Fig. 5c). These results are consistent with the prediction from the sensitivity analysis of the relative amplitude and phase for a simulation model with representative parameter values (Supplementary Text and Supplementary Fig. S4), in which the increased circadian expression of activator (simultaneous increase in both amplitude α_A and baseline γ_A) can decrease the relative amplitude of output oscillations (Fig. 5d), while not greatly affecting the output phase (Supplementary Fig. S4a, panels enclosed in the frame). Aside from the outliers (which are due to the greater expression of the activator), experimental data (Fig. 5b, coloured dots) matched the theoretical plot (Fig. 5b, black line), supporting the 'repressor-antiphasic-to-activator' mechanism for the relative amplitude.

This 'repressor-antiphasic-to-activator' mechanism is intuitive because it probably reflects the number of hours during which the activator can activate before the repressor begins to repress. However trivial it may seem, this intuitive repressor-antiphasic-to-activator mechanism is non-trivial and is even critical in generating higher-amplitude promoter activity in living cells, because no detectable oscillations are generated when a repressor is expressed in phase with an activator in various combinations (Supplementary Fig. S2d) or when an activator or repressor is expressed alone (Supplementary Fig. S2b).

Perturbation experiments of the natural transcriptional circuit in mammalian circadian clocks

One of the benefits and meanings of theoretical analysis is its formulation of a prediction that, if verified, leads us to a deeper understanding of the system in question. As discussed above, our simulation model with representative parameter values (see Supplementary Text) shows that an increase in circadian expression of an activator or repressor causes a decrease or an increase, respectively, in the relative amplitudes of the outputs (Fig. 5d). We reasoned that if (and only if) our simulation model could recapitulate the natural circadian system, it should be possible to apply the predictions derived from our simulation model to the natural transcriptional circuit in mammalian circadian clocks. To verify our predictions, we performed two perturbation experiments to increase the circadian expression of a natural activator, DBP, or repressor, E4BP4, by using p3 × E′-box-SV40-*Dbp* or p3 × RRE-SV40-*E4bp4*, respectively. As predicted, the relative amplitude of a natural downstream output from the D-box element, which is monitored by p3 × D-box-SV40-*dLuc*, is decreased (0.68-fold) or increased (1.76-fold) by the increase in circadian expression of activator or repressor, respectively (Fig. 5e). On the basis of these results, we concluded that both our simulation model and the derived design principles successfully recapitulated the natural transcriptional circuit in the mammalian circadian clocks.

DISCUSSION

In this study we successfully reconstructed two natural phases of the circadian clock (that is, daytime and night-time expression). The probability that any artificially generated peak will lie within 1 h of the naturally observed output peak is 2 in 24 (or 0.083) at best. The chance that two of two experiments would produce outputs within a 1 h difference from the targets is therefore $0.083 \times 0.083 = 0.0069$ (less than 0.05). Even if we adopt more stringent statistical criteria (the probability that two of three basic phases would be generated), the chance is (number of ways of selecting any 2 from 3) $\times 0.083 \times 0.083 \times (1 - 0.083) = 0.0191$ (less than 0.05). On the basis of these calculations, we conclude that our reconstruction of two natural phases in the circadian clock is statistically significant.

In this study we focused mainly on the competitive binding between transcription activators and repressors that control the phase and amplitude of the circadian output oscillations in mammalian circadian clocks. However, in the natural circadian clock systems of mammals and other organisms, transcription factors undergo various types of post-transcriptional regulation[9,22,32,34–42] such as modification and degradation, which may also contribute to the timing of the output phase and its amplitude. It will therefore be important in future to incorporate such post-transcriptional regulation into our *in cellulo* system to investigate its physical role in a circadian system. For example, it is already known that the VP16 polypeptide used in our *in cellulo* system is subject to ubiquitylation, which is important in transcriptional activation[47]. Once the VP16-specific ubiquitin ligase has been identified (it is as yet unidentified) it can be applied to our *in cellulo* system to investigate the impact of the post-transcriptional regulation on the circadian output oscillations.

In theory, the design principles described here for the phase and relative amplitude in mammalian circadian clocks can also be applied to the post-transcriptional regulation of transcription factors in mammals and other organisms, thereby allowing one to predict whether cyclic post-transcriptional regulation—depending on its phase—advances or delays the phase of the output, and whether it increases or decreases the relative amplitude of the output. For instance, the WC-1–WC-2 activator complex is expressed rhythmically by post-transcriptional regulation, whereas the *wc-1* and *wc-2* mRNAs in the *Neurospora* clock system are expressed constantly. The WC-1–WC-2 activator complex peaking at CT 17–18 and the FRQ repressor peaking at CT 8–10 drives many clock-controlled genes, and the overt rhythm in banding peaks at about CT 22 (refs 48, 49). This is quite consistent with the behaviour of our artificial circuit, in which an artificial night-time activator under RRE control (peaking at about CT 17–18) and a daytime repressor under D-box control (peaking at about CT 8) yield a high-amplitude circadian output whose phase is at CT 22.2—about 1.8 h before subjective dawn (Fig. 3a). This consistency implies a general applicability of the transcriptional logic that we describe in this study.

In summary, this study presents a synthetic approach to the 'proof-by-synthesis' of transcriptional logic. This approach provides us with a new strategy, not only to investigate the sufficiency of identified components of transcriptional circuits and their interactions, but also to reveal as yet unidentified components or interactions. For example, although we successfully (re)generated two basic phases, daytime and night-time, as well as additional phases near the subjective noon, dawn, dusk and late night, from the three basic circadian phases, we have not yet been able to regenerate one basic circadian phase, morning, which we expect to be regulated directly or indirectly by the three basic phases, to maintain circadian oscillations. Thus, in our *in cellulo* study, morning transcriptional regulation is still a 'missing link' in the mammalian clock system. Because a strong repressor at evening phase seems indispensable to the reconstruction of the morning phase, a candidate transcription factor could be CRY1, which is a transcriptional repressor expressed during the evening[4]. However, the expression regulation mechanism of the *Cry1* gene remains unknown because more than one DNA element seems involved in the expression[4]. Hence, the challenge of synthesizing evening and morning expression still lies ahead as we work towards the complete reconstruction of the transcriptional circuits underlying mammalian circadian clocks.

METHODS

Construction of plasmid pG4-*dLuc*, p3 × CCE-SV40-*dGAL4–VP16* and p3 × CCE-SV40-*dGal4*. To construct the output reporter plasmids, the pG5*Luc* (containing five UAS) plasmid in the CheckMate Mammalian Two-Hybrid system (Promega) was modified to contain four tandem repeats of the galactose UASs and a gene encoding destabilized luciferase (*dLuc*) as follows: pG5*Luc* was digested with *Eco*RI and *Nhe*I, blunted with T4 DNA polymerase, and ligated with itself. The product was then digested with *Sph*I and *Sal*I, ligated to the *Sph*I–*Sal*I fragment from the SV40-*dLuc* plasmid, containing the PEST sequence of *dLuc*[4], and termed pG4-*dLuc*. To construct activator or repressor plasmids, we modified the pBIND and pACT (Promega) vectors as follows. We amplified the *VP16* coding sequences from pACT (Promega) by PCR with a forward primer containing an *Eco*RV recognition sequence (5′-GATATCCTCGACGGCCCCCCCGACCG-3′) and a reverse primer containing a *Not*I recognition sequence (5′-GCGGCCGCTCTAGATGGCGATCCCGGACCCGGGGAATC-3′). The PCR product was then digested with *Eco*RV and *Not*I, and then fused to the *Gal4* gene in the pBIND vector.

A PEST fragment, amplified from the SV40-*dLuc* plasmid by PCR with forward (5′-ATGCGGTACCAGCCATGGCTTCCCGCCG-3′) and reverse (5′-CGTGGGTACCCACATTGATCCTAGCAGAAGC-3′) primers containing the *Kpn*I recognition sequence, was inserted into the *VP16*-fused and original pBIND vectors, previously digested with *Kpn*I. These products were termed pCMV-*dGAL4–VP16* and pCMV-*dGal4*, respectively. To drive the artificial activator or repressor in three basic circadian phases (morning, daytime or night-time), p3 × CCE-SV40-*dLuc* plasmids[4]—which contained the *Per2* E′-box (5′-gcgcgcgcggtCACGTTttccactatgtg acagcggagg-3′), the *Per3* D-box (5′-cccgcgcgTTATGTAAggtactcg-3′) or the *Bmal1* RRE (5′-aggcagAAAGTAGGTCAgggacg-3′) as a CCE (CCEs are indicated with underlines)—were digested with *Kpn*I and *Hin*dIII, blunted by T4 DNA polymerase, and inserted into the *Bgl*II and *Nhe*I site of pCMV-*dGAL4–VP16* or pCMV-*dGal4*. The end products, p3 × CCE-SV40-*dGAL4–VP16* and p3 × CCE-SV40-*dGal4*, were used as the activator or repressor plasmids for the artificial transcription circuits.

Real-time circadian reporter assays. Real-time circadian assays were performed as described previously[4,29], with the following modifications. NIH3T3 cells (American Type Culture Collection) were grown in DMEM medium (Invitrogen) supplemented with 10% FBS (JRH Biosciences) and antibiotics (25 U ml^{-1} penicillin, 25 mg ml^{-1} streptomycin; Invitrogen). At 24 h before transfection, cells were plated at 10^5 cells per well in 35-mm dishes. These cells were transfected with FuGene6 (Roche) in accordance with the manufacturer's instructions. The cells in each well were transfected with three plasmids (0.4 μg of *dLuc* reporter plasmid, 0.025 μg of p3 × CCE-SV40-*dGAL4–VP16* and 0.1 μg of p3 × CCE-SV40-*dGal4*). As the *dLuc* reporter plasmid we used p3 × CCE-SV40-*dLuc*[4] for monitoring the promoter activity of the artificial transcription factors, or pG4-*dLuc* for monitoring the transcriptional output in artificial transcriptional circuits. The amount of transfected plasmid was adjusted to 2.0 μg with empty vector. After 72 h, the medium in each well was replaced with 2 ml of culture medium (DMEM/10% FBS) supplemented with 10 mM HEPES (pH 7.2; Invitrogen), 0.1 mM luciferin (Promega), antibiotics and 0.01 μM forskolin (Nacalai Tesque). Bioluminescence was measured with photomultiplier tube detector assemblies (LM2400; Hamamatsu Photonics). The modules and cultures were maintained in a darkroom at 30 °C and interfaced with computers for continuous data acquisition. Photons were counted for 1 min at 12-min intervals.

Rhythmicity, period length and phase analysis of real-time bioluminescence data. The rhythmicity and period length of the promoter activity for each reporter were determined as described previously[29]. Bioluminescence time-series data were detrended by subtracting the trend curve of a 42 h timescale, calculated by the smoothing spline method with corresponding stiffness[29], and then used in the following analysis. Autocorrelation of the detrended time-series data was then calculated within the range 16–28 h to determine the circadian period of oscillation, which was defined to provide the strongest autocorrelation. Statistical significance (with $p = 0$ as most significant and $p = 1$ as least significant) of the circadian oscillation was evaluated by comparing the strongest autocorrelation of the detrended data within the range 16–28 h against that of white noise ($p < 0.01$). The periods of three *dLuc* reporters (two p3 × CCE-SV40-*dLuc* reporters for monitoring the promoter activity of the activator or repressor, and a pG4-*dLuc* reporter for monitoring the promoter activity of the output reporter) were calculated for each artificial circuit, and the mean value of the three periods was considered the 'circuit period.'

To calculate the normalized bioluminescence data (that is, the oscillatory component of the bioluminescence data) shown in Fig. 2c–d and Fig. 3a–d, the moving average of the absolute value of the detrended bioluminescence data was calculated first. The window size of the moving average was set to half of the circuit period calculated above. Then the oscillatory component of the detrended data was calculated by dividing the data by the moving average of the data at each time point. To calculate the peak time, a cosine curve was fitted to have maximum correlation with the normalized bioluminescence data. The peak time of the fitted cosine curve was used as the phase of each reporter.

Calculation of natural output phases of the E′-box, the D-box and the RRE. For comparison with the artificial output phases, the natural output phases controlled by the CCEs were determined as follows. NIH3T3 cells were transfected with p3 × CCE-SV40-*dLuc*, the *dLuc* gene being driven by the SV40 basic promoter fused with three tandem repeats of CCEs, and then monitored for 5 days for each CCE ($n = 25$–30). The means and standard deviations of the phase for the CCEs were 3.8 ± 0.84 (E′-box), 8.7 ± 1.13 (D-box) and 17.0 ± 0.81 (RRE) in CT, where we define CT 0 as the time of forskolin stimulation. These mean values were regarded as the natural output phases for the morning (E′-box), daytime (D-box) and night-time (RRE) elements in the experiments.

GeneChip expression data. The previously published genome-wide expression data for the liver[8] were re-analysed and re-annotated in this study, as described in detail in Supplementary Methods.

Theoretical model of the circadian circuit. Our theoretical model is based on the formula in our previous report[4] and has been extended to introduce basal transcription, degradation of mRNAs, and the translation and degradation of proteins to express the amount of the output proteins. The model comprises five formulas: the protein levels of the activator and repressor, the transcriptional activity of the output reporter, the mRNA level of the output reporter, and the protein level of the output reporter.

The protein levels of the activator and repressor are modelled as the sum of an oscillating component and a constant component. A formula for the protein level of an activator at time t is

$$A(t) \equiv \alpha_A \left(1 + \cos\left(2\pi \frac{t-\alpha}{24}\right)\right) + \gamma_A$$

where α_A, a and γ_A are the amplitude, phase and constant component of the activator, respectively. A formula for the protein level of a repressor at time t is

$$R(t) \equiv \alpha_R \left(1 + \cos\left(2\pi \frac{t-b}{24}\right)\right) + \gamma_R$$

where α_R, b and γ_R are the amplitude, phase and constant component of the repressor, respectively.

The transcriptional activity of an output reporter at time t is formulated as

$$T(t) \equiv V_1 \left(\frac{\left(\frac{A(t)}{K_A}\right)^n}{1 + \left(\frac{A(t)}{K_A}\right)^n + \left(\frac{R(t)}{K_R}\right)^n} + \beta \right)$$

where $1/K_A$ and $1/K_R$ are the strengths of the binding affinities of the activator and repressor, respectively. The constants K_A and K_R are inversely proportional to the strengths of the binding affinities (the larger the values of K_A and K_R, the weaker the binding), n is the Hill coefficient, β is the basal transcriptional activity and V_1 is the efficiency of transcription.

The mRNA and protein levels of an output reporter, $M(t)$ and $P(t)$, are modelled using differential equations, and formulated as

$$\frac{d}{dt} M(t) = T(t) - \left(\frac{\log 2}{T_1}\right) M(t)$$

$$\frac{d}{dt} P(t) = V_2 M(t) - \left(\frac{\log 2}{T_2}\right) P(t)$$

where V_2 is the efficiency of translation, and T_1 and T_2 are the half-life of the mRNA and protein, respectively.

Detailed information of the other experimental and computational methods is described in Supplementary Methods.

Note: Supplementary Information is available on the Nature Cell Biology website.

ACKNOWLEDGEMENTS

This research was supported by an intramural Grant-in-Aid from CDB (H.R.U.), the Uehara Memorial Foundation (H.R.U.) and KAKENHI (Grant-in-Aid for Scientific Research) on Priority Areas 'Systems Genomics' from the Ministry of Education, Culture, Sports, Science and Technology of Japan (H.R.U.). We thank Hideki Ukai for critical discussion, Rikuhiro G. Yamada and Tetsuya J. Kobayashi for programming the real-time bioluminescence data analysis, Yuichi Kumaki for the Promoter Database, and Erik A. Kuld, Douglas Sipp and Michael Royle for critical reading of the manuscript.

AUTHOR CONTRIBUTIONS

H.R.U. developed the concept of the proof-by-synthesis of the transcriptional logic underlying mammalian circadian clocks. M.U. constructed all materials used in this work and performed the real-time luminescence assays. T.K. developed the data analysis methods for the *in cellulo* and *in silico* data, and conducted these analyses. All the authors discussed the results and commented on the manuscript text.

COMPETING FINANCIAL INTERESTS

The authors declare no competing financial interests.

Published online at http://www.nature.com/naturecellbiology/
Reprints and permissions information is available online at http://npg.nature.com/reprintsandpermissions/

1. Hogenesch, J. B. *et al.* Characterization of a subset of the basic-helix–loop–helix-PAS superfamily that interacts with components of the dioxin signaling pathway. *J. Biol. Chem.* **272,** 8581–8593 (1997).
2. Gekakis, N. Role of the CLOCK protein in the mammalian circadian mechanism. *Science* **280,** 1564–1569 (1998).
3. Yoo, S. H. *et al.* A noncanonical E-box enhancer drives mouse Period2 circadian oscillations *in vivo*. *Proc. Natl Acad. Sci. USA* **102,** 2608–2613 (2005).
4. Ueda, H. R. *et al.* System-level identification of transcriptional circuits underlying mammalian circadian clocks. *Nature Genet.* **37,** 187–192 (2005).
5. Falvey, E., Marcacci, L. & Schibler, U. DNA-binding specificity of PAR and C/EBP leucine zipper proteins: a single amino acid substitution in the C/EBP DNA-binding domain confers PAR-like specificity to C/EBP. *Biol. Chem.* **377,** 797–809 (1996).
6. Harding, H. P. & Lazar, M. A. The orphan receptor Rev-ErbAα activates transcription via a novel response element. *Mol. Cell. Biol.* **13,** 3113–3121 (1993).
7. Preitner, N. The orphan nuclear receptor REV-ERBα controls circadian transcription within the positive limb of the mammalian circadian oscillator. *Cell* **110,** 251–260 (2002).
8. Ueda, H. R. *et al.* A transcription factor response element for gene expression during circadian night. *Nature* **418,** 534–539 (2002).
9. Reppert, S. M. & Weaver, D. R. Coordination of circadian timing in mammals. *Nature* **418,** 935–941 (2002).
10. Bunger, M. K. Mop3 is an essential component of the master circadian pacemaker in mammals. *Cell* **103,** 1009–1017 (2000).
11. King, D. P. Positional cloning of the mouse circadian clock gene. *Cell* **89,** 641–653 (1997).
12. Reick, M., Garcia, J. A., Dudley, C. & McKnight, S. L. NPAS2: an analog of clock operative in the mammalian forebrain. *Science* **293,** 506–509 (2001).
13. Okano, T., Sasaki, M. & Fukada, Y. Cloning of mouse BMAL2 and its daily expression profile in the suprachiasmatic nucleus: a remarkable acceleration of Bmal2 sequence divergence after *Bmal* gene duplication. *Neurosci. Lett.* **300,** 111–114 (2001).
14. Zheng, B. *et al.* The *mPer2* gene encodes a functional component of the mammalian circadian clock. *Nature* **400,** 169–173 (1999).
15. Shearman, L. P., Jin, X., Lee, C., Reppert, S. M. & Weaver, D. R. Targeted disruption of the *mPer3* gene: subtle effects on circadian clock function. *Mol. Cell. Biol.* **20,** 6269–6275 (2000).
16. Zheng, B. Nonredundant roles of the *mPer1* and *mPer2* genes in the mammalian circadian clock. *Cell* **105,** 683–694 (2001).
17. Cermakian, N., Monaco, L., Pando, M. P., Dierich, A. & Sassone-Corsi, P. Altered behavioral rhythms and clock gene expression in mice with a targeted mutation in the *Period1* gene. *EMBO J.* **20,** 3967–3974 (2001).
18. Bae, K. Differential functions of mPer1, mPer2, and mPer3 in the SCN circadian clock. *Neuron* **30,** 525–536 (2001).
19. van der Horst, G. T. Mammalian Cry1 and Cry2 are essential for maintenance of circadian rhythms. *Nature* **398,** 627–630 (1999).
20. Vitaterna, M. H. *et al.* Differential regulation of mammalian period genes and circadian rhythmicity by cryptochromes 1 and 2. *Proc. Natl Acad. Sci. USA* **96,** 12114–12119 (1999).
21. Honma, S. Dec1 and Dec2 are regulators of the mammalian molecular clock. *Nature* **419,** 841–844 (2002).
22. Lowrey, P. L. Positional syntenic cloning and functional characterization of the mammalian circadian mutation tau. *Science* **288,** 483–491 (2000).
23. Xu, Y. *et al.* Functional consequences of a CKIδ mutation causing familial advanced sleep phase syndrome. *Nature* **434,** 640–644 (2005).
24. Lavery, D. J. *et al.* Circadian expression of the steroid 15 α-hydroxylase (Cyp2a4) and coumarin 7-hydroxylase (Cyp2a5) genes in mouse liver is regulated by the PAR leucine zipper transcription factor DBP. *Mol. Cell. Biol.* **19,** 6488–6499 (1999).
25. Gachon, F. *et al.* The loss of circadian PAR bZip transcription factors results in epilepsy. *Genes Dev.* **18,** 1397–1412 (2004).
26. Mitsui, S., Yamaguchi, S., Matsuo, T., Ishida, Y. & Okamura, H. Antagonistic role of E4BP4 and PAR proteins in the circadian oscillatory mechanism. *Genes Dev.* **15,** 995–1006 (2001).
27. Sato, T. K. A functional genomics strategy reveals Rora as a component of the mammalian circadian clock. *Neuron* **43,** 527–537 (2004).
28. André, E. *et al.* Disruption of retinoid-related orphan receptor β changes circadian behavior, causes retinal degeneration and leads to vacillans phenotype in mice. *EMBO J.* **17,** 3867–3877 (1998).
29. Sato, T. K. *et al.* Feedback repression is required for mammalian circadian clock function. *Nature Genet.* **38,** 312–319 (2006).
30. Akashi, M. & Takumi, T. The orphan nuclear receptor RORα regulates circadian transcription of the mammalian core-clock Bmal1. *Nature Struct. Mol. Biol.* **12,** 441–448 (2005).
31. Sadowski, I., Ma, J., Triezenberg, S. & Ptashne, M. GAL4–VP16 is an unusually potent transcriptional activator. *Nature* **335,** 563–564 (1988).
32. Gallego, M. & Virshup, D. M. Post-translational modifications regulate the ticking of the circadian clock. *Nature Rev. Mol. Cell Biol.* **8,** 139–148 (2007).
33. Kojima, S., Hirose, M., Tokunaga, K., Sakaki, Y. & Tei, H. Structural and functional analysis of 3′ untranslated region of mouse *Period1* mRNA. *Biochem. Biophys. Res. Commun.* **301,** 1–7 (2003).
34. Lee, C., Etchegaray, J., Cagampang, F. R., Loudon, A. S. & Reppert, S. M. Posttranslational mechanisms regulate the mammalian circadian clock. *Cell* **107,** 855–867 (2001).
35. Eide, E. J., Vielhaber, E. L., Hinz, W. A. & Virshup, D. M. The circadian regulatory proteins BMAL1 and cryptochromes are substrates of casein kinase Iepsilon. *J. Biol. Chem.* **277,** 17248–17254 (2002).
36. Sanada, K., Okano, T. & Fukada, Y. Mitogen-activated protein kinase phosphorylates and negatively regulates basic helix–loop–helix-PAS transcription factor BMAL1. *J. Biol. Chem.* **277,** 267–271 (2002).
37. Toh, K. L. *et al.* An hPer2 phosphorylation site mutation in familial advanced sleep phase syndrome. *Science* **291,** 1040–1043 (2001).
38. Yin, L., Wang, J., Klein, P. S. & Lazar, M. A. Nuclear receptor Rev-erbα is a critical lithium-sensitive component of the circadian clock. *Science* **311,** 1002–1005 (2006).
39. Akashi, M., Tsuchiya, Y., Yoshino, T. & Nishida, E. Control of intracellular dynamics of mammalian period proteins by casein kinase I ε (CKIε) and CKIδ in cultured cells. *Mol. Cell. Biol.* **22,** 1693–1703 (2002).
40. Yagita, K. *et al.* Nucleocytoplasmic shuttling and mCRY-dependent inhibition of ubiquitylation of the mPER2 clock protein. *EMBO J.* **21,** 1301–1314 (2002).
41. Cardone, L. *et al.* Circadian clock control by SUMOylation of BMAL1. *Science* **309,** 1390–1394 (2005).
42. Vielhaber, E. L., Duricka, D., Ullman, K. S. & Virshup, D. M. Nuclear export of mammalian PERIOD proteins. *J. Biol. Chem.* **276,** 45921–45927 (2001).
43. Ripperger, J. A. & Schibler, U. Rhythmic CLOCK-BMAL1 binding to multiple E-box motifs drives circadian Dbp transcription and chromatin transitions. *Nature Genet.* **38,** 369–374 (2006).
44. Akhtar, R. A. *et al.* Circadian cycling of the mouse liver transcriptome, as revealed by cDNA microarray, is driven by the suprachiasmatic nucleus. *Curr. Biol.* **12,** 540–550 (2002).
45. Panda, S. *et al.* Coordinated transcription of key pathways in the mouse by the circadian clock. *Cell* **109,** 307–320 (2002).
46. Storch, K. F. *et al.* Extensive and divergent circadian gene expression in liver and heart. *Nature* **417,** 78–83 (2002).
47. Salghetti, S. E., Caudy, A. A., Chenoweth, J. G. & Tansey, W. P. Regulation of transcriptional activation domain function by ubiquitin. *Science* **293,** 1651–1653 (2001).
48. Lee, K., Loros, J. J. & Dunlap, J. C. Interconnected feedback loops in the *Neurospora* circadian system. *Science* **289,** 107–110 (2000).
49. Dunlap, J. C. *et al.* A circadian clock in *Neurospora*: how genes and proteins cooperate to produce a sustained, entrainable, and compensated biological oscillator with a period of about a day. *Cold Spring Harb. Symp. Quant. Biol.* **72,** 57–68 (2007).

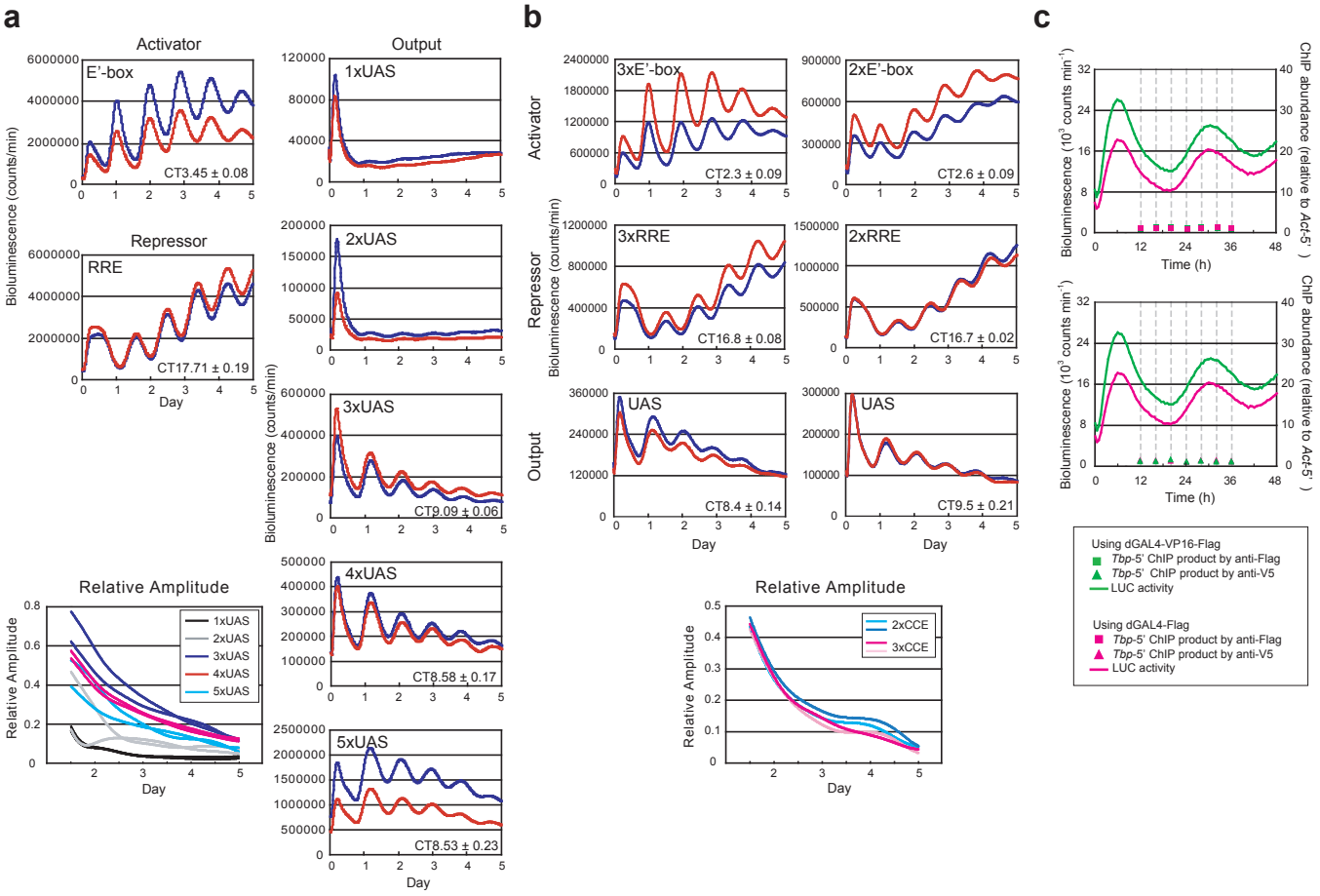

Figure S1 Evaluating our *in cellulo* mammalian cell culture system. **a,** Determination of number of UASs in the artificial promoter to regulate the output reporter gene. We first constructed reporter vectors, varying the number of UAS (from 1 through 5) on the promoter driving a reporter gene (*dLuc*). We transfected them with a morning activator and a night-time repressor into NIH3T3 cells and then monitored the bioluminescence from the cells. The raw bioluminescence data from two independent samples are shown. The relative amplitudes of each output signal from two independent samples are also shown (**lower left panel**). **b,** Determination of number of CCEs in the artificial promoter to regulate the activator and repressor genes. We first constructed two sets of vectors with two and three copies of the clock-controlled elements (CCE; E'-box from the *Per2* gene, or RRE from the *Bmal1* gene) on promoters driving a reporter gene (*dLuc*), an artificial activator gene (*dGal4-VP16*) or an artificial repressor gene (*dGal4*). We then monitored their promoter activities (either 2× or 3× E'-box, and either 2× or 3× RRE) as well as the output (UAS) from artificial transcriptional circuits with a morning activator and a night-time repressor. The raw bioluminescence data from two independent samples are shown. The relative amplitudes of each output signal from two independent samples are also shown (**lower left panel**). **c,** Negative controls for quantification of GAL4-VP16-FLAG and GAL4-FLAG bindings to the UAS in the artificial transcriptional circuits. After normalization for the amount of input DNA, the amount of *Tbp* promoter (*Tbp*-5') region immunoprecipitated by anti-FLAG antibody (squares) and by anti-V5 antibody (triangles) were quantified relative to a constitutively unbound region (*Act*-5'). These relative amounts of *Tbp*-5' ChIP products are indicated along with the LUC activity (line) for two different artificial transcriptional circuits using dGAL4-VP16-FLAG (green) and dGAL4-FLAG (magenta). ChIP assays were performed with the artificial transcriptional circuit (morning activator and night-time repressor) in NIH3T3 cells at 4-h intervals for 24 h with anti-FLAG antibody and anti-V5 antibody as negative control.

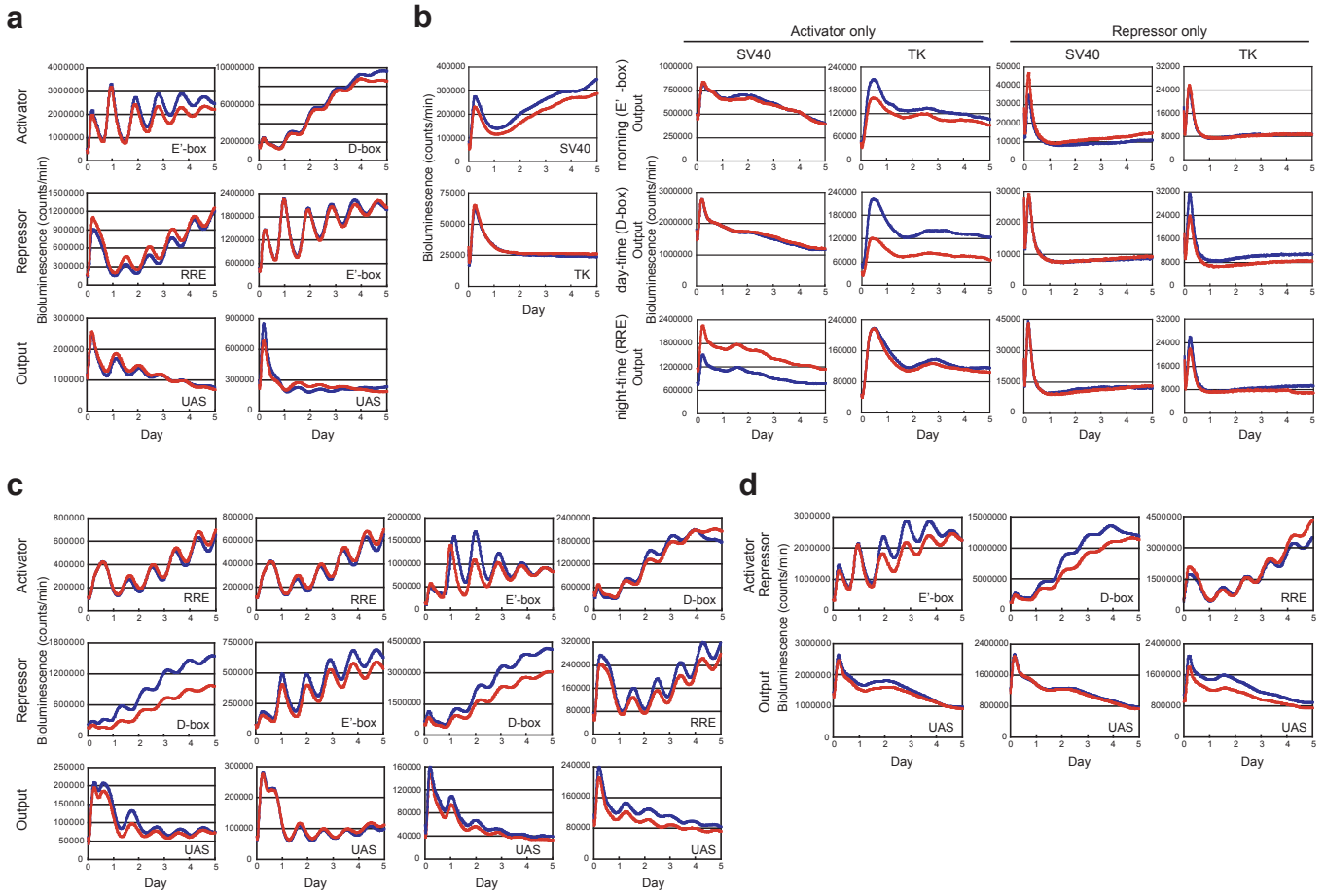

Figure S2 Raw bioluminescence data from artificial transcriptional circuits with various combinations of activators and repressors. **a,** Synthesis of day-time and night-time expressions in two different artificial transcriptional circuits. Promoter activities of an activator, repressor, and output reporter in two different artificial transcriptional circuits: (**left**) morning activator under E'-box control and night-time repressor under RRE control, and (**right**) day-time activator under D-box control and morning repressor under E'-box control. **b,** High-amplitude transcriptional oscillation cannot be generated by an activator or a repressor alone. (**left**) The activities of the SV40 promoter and thymidine kinase (TK) promoter. The promoter activities were monitored by bioluminescence from NIH3T3 cells, which were transfected SV40-*dLuc* and TK-*dLuc*. The transcriptional activity of TK promoter indicates lower expression than SV40 promoter (1:7.28 ± 0.70). (**right**) Promoter activities of the output reporter in six different artificial transcriptional circuits. The promoters used to regulate the activator and repressor genes were SV40 promoter (SV40, **left panels**) and TK promoter (TK, **right panels**): morning activator or repressor alone (**upper panels**), day-time activator or repressor alone (**middle panels**) and night-time activator or repressor alone (**lower panels**). **c,** Synthesis of various phases from three basic circadian phases in artificial transcriptional circuits. Promoter activities of an activator, a repressor, and an output reporter in four different artificial transcriptional circuits: (**left**) night-time activator under RRE control and day-time repressor under D-box control, (**middle left**) night-time activator under RRE control and morning repressor under E'-box control: (**middle right**) morning activator under E'-box control and day-time repressor under D-box control: and (**right**) day-time activator under D-box control and night-time repressor under RRE control. **d,** Promoter activity in artificial transcriptional circuits with a repressor in phase with an activator. Promoter activities of an activator, repressor, and output reporter in three different artificial transcriptional circuits: (**left**) morning activator and repressor both under E'-box control: (**middle**) day-time activator and repressor both under D-box control: and (**right**) night-time activator and repressor both under RRE control. The raw bioluminescence data from two independent samples are shown.

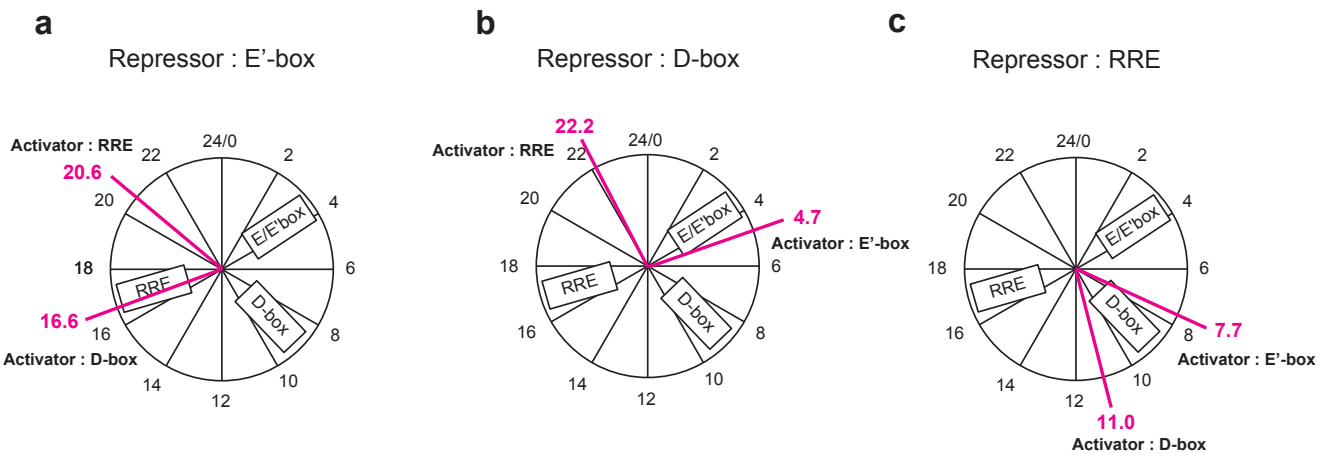

Figure S3 Transcriptional mechanisms to generate novel phases. Output phases in artificial transcriptional circuits with a morning repressor (**a**), day-time repressor (**b**), or night-time repressor (**c**). The phase of an output reporter (magenta lines and numbers) is indicated in circadian time (h) with the activator used (bold black). In artificial transcriptional circuits *in cellulo*, the output phase could be changed according to the input phase of the activator, even if that of the repressor was unchanged.

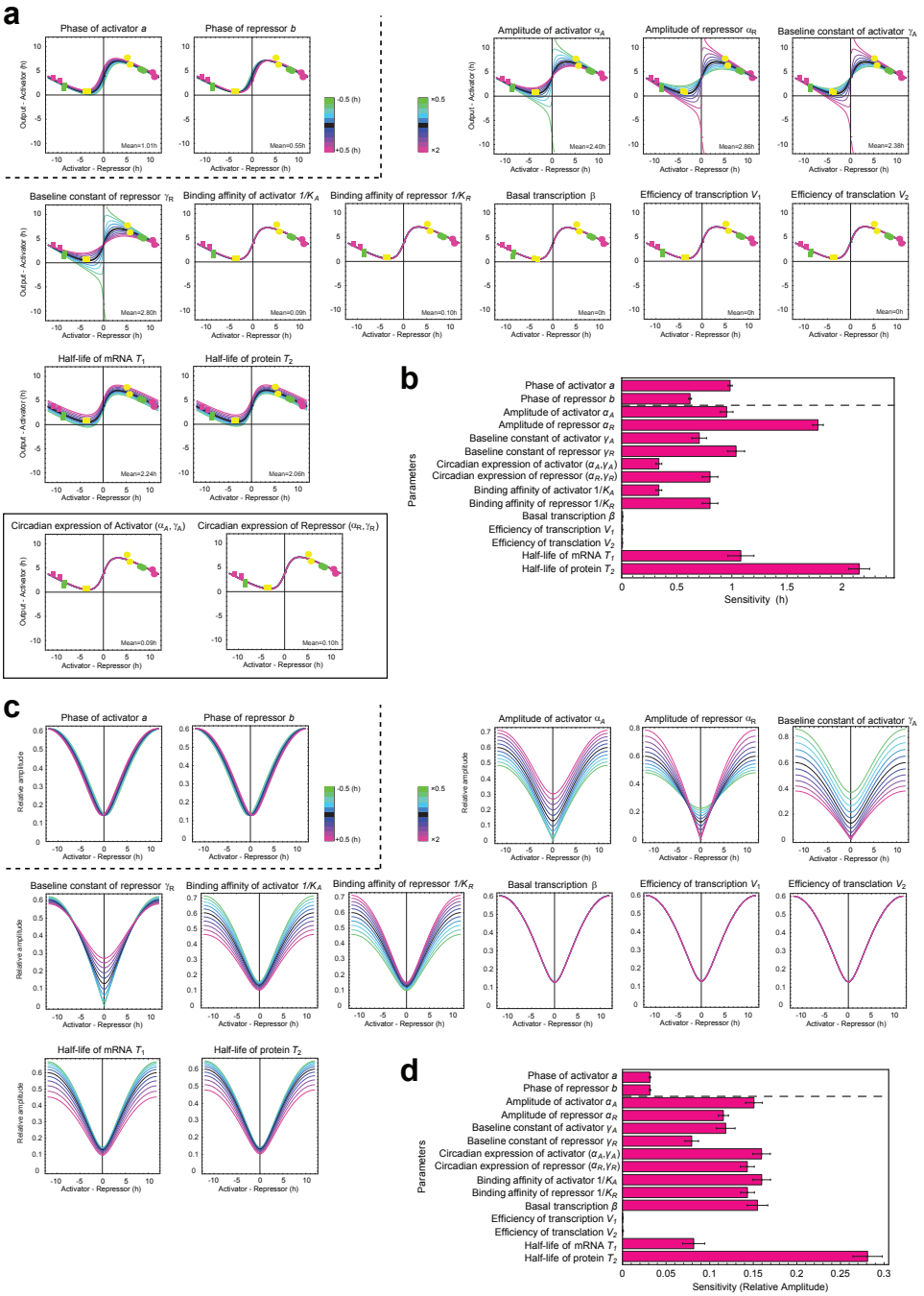

Figure S4 Sensitivity of the output phase and the relative amplitude to each parameter. **a**, The sensitivity of the output phase over -12 < *a*-*b* < 12 is shown when each parameter value was changed by 1 hour (*a* and *b*) or 4-fold (the others). X-axis represents the advance of a repressor compared to an activator (h) (phase difference between an activator and repressor), while Y-axis represents the delay of an output reporter compared to an activator (h) (phase difference between an output reporter and activator). The effects of simultaneous increases in both absolute amplitude and base-line levels of an input activator (α_A and γ_A) or repressor (α_R and γ_R) are also shown in the boxed-panel (**inbox**). The black curve shows a simulation model with representative parameter values of one hundred fitted parameter sets; the other curves show changed values for sensitive analysis. **b**, The simulated sensitivity of the output phase to the parameter describing each process. Each bar shows the average phase difference obtained by changing its original parameter value by 1 hour (parameter *a* and *b*) or 4-fold (other parameters). Each error bar represents standard error. These values were calculated from 100 simulations with trimming of the 5% outliers. **c**, The sensitivity of the relative amplitude over -12 < *a*-*b* < 12 is shown when each parameter value was changed by 1 hour (*a* and *b*) or 4-fold (the others). X-axis represents the advance of a repressor compared to an activator (h) (phase difference between an activator and repressor), while Y-axis represents the relative amplitude of oscillation of output protein (dLUC) activity. The black curve shows a simulation model with representative parameter values of one hundred fitted parameter sets; the other curves show changed values for sensitive analysis. **d**, The simulated sensitivity of the relative amplitude to the parameter describing each process. Each bar shows the average relative amplitude difference obtained by changing its original parameter value by 1 hour (parameter *a* and *b*) or 4-fold (other parameters). Each error bar represents standard error. These values were calculated from 100 simulations with trimming of the 5% outliers.

Supplementary Text

Determination of number of the galactose upstream activating sequences.

The number of the galactose upstream activating sequences (UASs) was determined by the following experiments. We constructed reporter vectors with varying numbers of UAS (from 1 through 5) on the promoter driving *dLuc* output, reporter, transfected the vector into NIH3T3 cells and then monitored bioluminescence from the transfected cells (**Supplementary Fig. 1a**). We observed that reporter vectors with 1 or 2×UAS did not exhibit high-amplitude oscillations, while those with 3, 4, and 5×UAS produced high-amplitude oscillations in comparable phases. In this manuscript, we adopt 4×UAS because outputs with 4×UAS results in the relative amplitudes with the smallest variation (**Supplementary Fig. 1a lower left**).

Determination of number of the clock-controlled elements.

To determine the number of clock-controlled elements (CCE) that we should use to drive activator/repressor expression, we constructed two sets of vectors containing either two or three copies of the CCEs on promoters driving *dLuc* reporter or artificial activators/repressors, and monitored their promoter activities and transcriptional output (**Supplementary Fig. 1b**). Via bioluminescence, we observed that promoter activities and outputs for both 2 and 3×CCE exhibited comparable phases and relative amplitudes (**Supplementary Fig. 1b lower left**). Although we could have used 2xCCE, we opted to use 3×CCE in our system, because it has been the construct used since our preceding works[1].

Comparison of the previous predictions and the numerical experimental data

The predictions of repressor-antiphasic-to-activator and repressor-precedes-activator mechanisms in the previous report[1] is well matched with our numerical experimental data although we should give attention to the difference of the transcription activity that was evaluated in the previous model and the output protein activities that were measured in our experiment. Due to transcription and translation of an output reporter, the simulation model with representative parameter values (**black line** in **Fig. 5a**) in our current manuscript has an approximately 4-hour delay from the previous model. This delay is comparable to the delay estimated from our experiment in **Fig. 2a** and **b**, where the peak-time of dGAL4-VP16 binding to UAS and peak-time of *Luciferase* mRNA are about 3.0-hour and 2.0-hour before that of output *Luciferase* activity, respectively, and thus the delay between transcription activity and output protein was estimated as about 2.0–3.0 hours.

Sensitivity analysis of the phase and relative amplitude of the output oscillations

We calculated the sensitivity of the phase and the relative amplitude of the output oscillation to each parameter by changing the parameter's value by 4-fold (from 1/2- to 2-times the original parameter value) (**Supplementary Fig. 4a, c**), *except* for the input phase of the transcriptional factors, which we changed by 1 h (from a 0.5-h delay to 0.5-h in advance of the original phase). By repeating this procedure for 100 fitted parameter sets, we also evaluated the average contribution of each process (**Supplementary Fig. 4b, d**).

As expected from our *in cellulo* mammalian cell culture system results (**Figs. 4a-c**), the phase difference of input transcription factors can contribute to the output phase *in silico* (**Supplementary Fig. 4b**). For example, a 1-h alteration in the phase of an activator or a repressor led to ~1 h changes in the output phase (0.98 h for a and 0.62 h for b). In addition, the absolute amplitude and base-line level of the input transcription factor phases contributed to the output phase: a 4-fold parameter change in the absolute amplitude (α_A and α_R) or the absolute base-line level (γ_A and γ_R) of an activator or repressor could alter the output phase by 1 ~ 2 h (0.95 h for α_A, 1.77 h for α_R, 0.70 h for γ_A and 1.03 h for γ_R). However, the effects of absolute amplitudes and base-line levels on output phase seemed to cancel out when they were both increased simultaneously. This was because the effects of simultaneous increases of *both* absolute amplitude and base-line levels of the inputs are smaller than *independent* increases in absolute amplitude *or* base-line levels (0.33 h for α_A and γ_A, and 0.80 h for α_R and γ_R and see also **Supplementary Fig. 4a inbox**). We noted that binding affinities of the input activator or repressor onto the promoters ($1/K_A$, or $1/K_R$) are theoretically equivalent to the simultaneous increase of α_A and γ_A, or α_R and γ_R, respectively (0.33 h for $1/K_A$ and 0.80 h for $1/K_R$). We also noted that the half-life of the mRNA or protein of a reporter (1.07 h for T_1 and 2.14 h for T_2) contributed more to the output phase than the reporter's transcription or translation processes (<0.01 h for β, V_1 and V_2), which implies that the degradation process can cause output phases to be fairly continuous, as is observed *in vivo*[2-5].

As for the contribution of input transcription factors to the relative amplitude of the output oscillations (**Supplementary Fig. 4d**), we find that the absolute amplitudes and base-line levels of the inputs have larger effects than the phases of the inputs (0.15 for α_A, 0.12 for α_R, 0.12 for γ_A and 0.08 for γ_R, 0.03 for a, 0.03 h for b). Interestingly, these effects of absolute amplitudes and base-line levels of the inputs do not seem to

cancel out much when both are increased simultaneously since the effects of simultaneous increase of *both* absolute amplitude and base-line levels of the inputs are similar to, or greater than, those of *either* absolute amplitude or base-line levels of the inputs (0.16 for α_A and γ_A, and 0.14 for α_R and γ_R and see also **Fig. 5d**). Hence, we observe a marked contrast to the output phase, implying that absolute circadian expression levels of the inputs seem to play a key role in controlling the relative amplitudes of outputs.

To recap, we noted: 1) that binding affinity of the input activator or repressor onto the promoters ($1/K_A$, or $1/K_R$) are theoretically equivalent to the simultaneous increase of α_A and γ_A, or α_R and γ_R, respectively (0.16 for $1/K_A$ and 0.14 for $1/K_R$), and; 2) that the half-life of the mRNA or protein of a reporter (0.08 for T_1 and 0.28 h for T_2) also contributed to the relative amplitude of the output Interestingly, however, basal transcription is more important for the relative amplitude of the output than the efficiencies of transcription and translation (0.15 for β, <0.001 for V_1 and V_2).

Supplementary Methods

Construction of pCMV-*dGal4-VP16-Flag* and pCMV-*dGal4-Flag*. To construct *Flag*-tagged activator and repressor plasmids regulated by CMV promoter, the *Flag*-PEST coding DNA fragment, amplified from the pCMV-*dGal4* plasmid (See **Methods** in main text) by PCR with forward (5'-GGCCGCAGGTACC*GACTACAAGGATGACGATGACAAG*AGCCATGGCTTCCC GCCGGCGGTG-3') and reverse (5'-TTATTCAGGTACCCACATTGATCCTAGCAGAAGC-3') primers containing the *Kpn*I recognition sequence (under line) and *Flag* coding sequence (italics), was inserted into the *VP16*-fused and original pBIND vectors (Promega, See **Methods** in main text), previously digested with *Kpn*I. These products were termed pCMV-*dGal4-VP16-Flag* and pCMV-*dGal4-Flag*, respectively, and used for Western Blot analysis.

Measurement of protein half-lives of dGAL4-VP16-FLAG and dGAL4-FLAG. NIH3T3 cells (American Type Culture Collection) were grown in DMEM (Invitrogen) supplemented with 10% FBS (JRH Biosciences) and antibiotics (25 U/ml penicillin, 25 mg/ml streptomycin; Invitrogen). Cells were plated at 1×10^6 cells per dish in 90-mm dishes 24 h before transfection. These cells were transfected with FuGene6 (Roche) according to the manufacturer's instructions. The cells in each well were transfected with 12 μg of pCMV-*dGal4-VP16-Flag* or pCMV-*dGal4-Flag*. After 24 h, the cells in each well were harvested and plated in 6 35-mm dishes. After 48 h, the cells were treated with cycloheximide (CHX, SIGMA) at a final concentration of 100 μg/ml until their harvest. The treated cells were harvested at 0, 2, 4 and 6 h and used for Western Blot Analysis.

For Western Blot Analysis, each nuclear and cytoplasmic fraction was extracted from the harvested cells with NE-PER Nuclear and Cytoplasmic Extraction Reagents (PIERCE). Each cell lysate was applied to a lane of polyacrylamide gels. For immunoblot analysis, proteins were transferred to PVDF membranes. Anti-FLAG M2 monoclonal Antibody-Peroxidase Conjugate (SIGMA) was diluted 2000-fold and used for detection of dGAL4-VP16-FLAG and dGAL4-FLAG protein. Anti-Tubulinα monoclonal antibody (clone DM1A, LAB VISION) was diluted 330-fold, and used for detection of Tubulinα protein as internal control. For visualization, ECL Plus Western Blotting Detection System (GE Healthcare) and LAS-1000 (FUJIFILM) were used according to the manufacturer's instructions.

Construction of plasmid pG1-*dLuc*, pG2-*dLuc*, pG3-*dLuc and pG5-dLuc*. To construct the output reporter plasmids, the pG5*Luc* (containing five UAS) plasmid in the CheckMate Mammalian Two-Hybrid system (Promega) was modified to contain one, two or three tandem repeats of the galactose upstream activating sequences (UAS) and a gene encoding destabilized luciferase (*dLuc*) as follows. pG5*Luc* was digested with *Xba*I (partial digestion) and *EcoR*I (for remaining one UAS), *Xho*I and *Nhe*I (for remaining two UAS), or *Xho*I and *EcoR*I (for remaining three UAS). These digested vectors were blunted by T4 DNA Polymerase, and ligated with itself. The products and pG5*Luc* (Promega) were then digested with *Sph*I and *Sal*I, ligated to the *Sph*I-*Sal*I fragment from the SV40-*dLuc* plasmid, which contains the PEST sequence of the *dLuc*[1] and termed pG1-*dLuc* (containing one UAS), pG2-*dLuc* (containing two UAS), pG3-*dLuc* (containing three UAS), and pG5- *dLuc* (containing five UAS). These constructs were used as the reporter plasmids for the artificial transcription circuits.

Real-time circadian reporter assays using reporter vectors with UAS (1-5×). Real-time circadian assays were performed as previously described[1,6] with the following modifications. NIH3T3 cells (American Type Culture Collection) were grown in DMEM (Invitrogen) supplemented with 10% FBS (JRH Biosciences) and antibiotics (25 U/ml penicillin, 25 mg/ml streptomycin; Invitrogen). Cells were plated at 1×10^5 cells per well in 35-mm dishes 24 h before transfection. These cells were transfected with FuGene6 (Roche) according to the manufacturer's instructions. The cells in each well were transfected with three plasmids (0.4 μg of *dLuc* reporter plasmid, 0.025 μg of p3×E'-box-SV40-*dGal4-VP16*, and 0.1 μg of p3×RRE-SV40-*dGal4*). As the *dLuc* reporter plasmid, we used p3×E'-box-SV40-*dLuc* and p3×RRE-SV40-*dLuc*[1] for monitoring the promoter activity of the artificial transcription factors, or pG1-*dLuc,* pG2-*dLuc,* pG3-*dLuc,* pG4-*dLuc* , and pG5-*dLuc* for monitoring the transcriptional output in the artificial transcriptional circuits. The amount of transfected plasmid was adjusted to 2.0 μg with empty vector. After 72 h, the media in each well was replaced with 2 ml of culture medium (DMEM/10% FBS) supplemented with 10 mM HEPES (pH 7.2, Invitrogen), 0.1 mM luciferin (Promega), antibiotics, and 0.01 μM forskolin (Nacalai Tesque). Bioluminescence was measured with photomultiplier tube (PMT) detector assemblies (LM2400, Hamamatsu Photonics). The modules and cultures were maintained in a darkroom at 30°C and interfaced with computers for continuous data acquisition. Photons were counted for 1 min at 12-min intervals.

Construction of plasmid p2×CCE-SV40-*dLuc,* p2×CCE-SV40-*dGal4-VP16* and p2×CCE-SV40-*dGal4*. To construct activator or repressor plasmids regulated by two tandem repeated clock-controlled element (CCE), we modified the pCMV-*dGal4-VP16* or pCMV-*dGal4* vectors as follows. The oligonucleotides containing two tandem repeat sequences of CCEs were annealed, and inserted into *Mlu*I/*Bgl*II site of the

SV40-*dLuc* vectors[1]. These products (p2×CCE-SV40-*dLuc* plasmids) were digested with *Kpn*I and *Hin*dIII, blunted by T4 DNA polymerase, and inserted into the *Bgl*II and *Nhe*I site of pCMV-*dGal4-VP16* or pCMV-*dGal4*. The end products, p2×CCE-SV40-*dGal4-VP16* or p2×CCE-SV40-*dGal4*, and the intermediate product p2×CCE-SV40-*dLuc* were used as the activator or repressor plasmids for the artificial transcription circuits, and as the reporter plasmid for promoter activity, respectively.

The oligonucleotide sequence for two tandem repeated clock-controlled element.

2× *Per2* E'-box-forward:
5'-CGCGGCGCGCGCGGTCACGTTTTCCACTATGTGACAGCGGAGGGCGCGCG
CGGTCACGTTTTCCACTATGTGACAGCGGAGG-3'

2× *Per2* E'-box-reverse:
5'-GATCCCTCCGCTGTCACATAGTGGAAAACGTGACCGCGCGCGCCCTCCGC
TGTCACATAGTGGAAAACGTGACCGCGCGCGC-3'

2× *Bmal1* RRE-forward:
5'-CGCGAGGCAGAAAGTAGGTCAGGGACGAGGCAGAAAGTAGGTCAGGGA
CG-3'

2× *Bmal1* RRE-reverse:
5'-GATCCGTCCCTGACCTACTTTCTGCCTCGTCCCTGACCTACTTTCTGCCT-3'

Real-time circadian reporter assays using artificial activator and repressor derived by 2×CCE-SV40 promoters. Real-time circadian assays were performed as previously described[1,6] and as mentioned above with the following modifications.

NIH3T3 cells were plated at 1×10^5 cells per well in 35-mm dishes 24 h before transfection, and were transfected with FuGene6. The cells in each well were transfected with three plasmids (0.4 μg of *dLuc* reporter plasmid, 0.025 μg of p2×E'-box-SV40-*dGal4-VP16*, and 0.1 μg of p2×RRE-SV40-*dGal4*). As the *dLuc* reporter plasmid, we used p2×E'-box-SV40-*dLuc* and p3×RRE-SV40-*dLuc*[1] for monitoring the promoter activity of the artificial transcription factors, and pG4-*dLuc* for monitoring the transcriptional output in artificial transcriptional circuits. The amount of transfected plasmid was adjusted to 2.0 μg with empty vector. After 72 h, the media in each well was replaced with 2 ml of culture medium including 0.01 μM forskolin. Bioluminescence was measured with photomultiplier tube (PMT) detector assemblies (LM2400) in a darkroom at 30°C.

Construction of p3×E'-box-SV40-*dGal4-VP16-Flag* and p3×RRE-SV40-*dGal4-Flag*. To construct *Flag*-tagged activator and repressor plasmids regulated by E'-box and RRE, the *Flag*-PEST coding DNA fragment, amplified from the pCMV-*dGal4* plasmid (See **Methods** in main text) by PCR with forward (5'-GGCCGCAGGTACC*GACTACAAGGATGACGATGACAAG*AGCCATGGCTTCCCGCCGGCGGTG-3') and reverse (5'-TTATTCAGGTACCCACATTGATCCTAGCAGAAGC-3') primers containing the *Kpn*I recognition sequence (under line) and *Flag* sequence (italics), was inserted into the *Kpn*I sites of p3×E'-box-SV40-*dGal4-VP16* and p3×RRE-SV40-*dGal4* vectors (See **Methods** in main text), that were previously digested with *Kpn*I. These products were termed p3×E'-box-SV40-*dGal4-VP16-Flag* and p3×RRE-SV40-*dGal4-Flag*, and used for Chromatin Immunoprecipitation assay.

Chromatin Immunoprecipitation (ChIP) assay and Quantitative PCR of ChIP pruduct. NIH3T3 cells (American Type Culture Collection) were grown in DMEM (Invitrogen) supplemented with 10% FBS (JRH Biosciences) and antibiotics (25 U/ml penicillin, 25 mg/ml streptomycin; Invitrogen). Cells were plated at 1×10^6 cells per dish in 14 90-mm dishes 24 h before transfection. These cells were transfected with FuGene6 (Roche) according to the manufacturer's instructions. The cells in each dish were transfected with three plasmids ({8 μg of pG4-*dLuc*, 4.8 μg of p3×E'-box-SV40-*dGal4-VP16-Flag* and 19.2 μg of p3×RRE-SV40-*dGal4*} and {8 μg of pG4-*dLuc*, 4.8 μg of p3×E'-box-SV40-*dGal4-VP16* and 19.2 μg of p3×RRE-SV40-*dGal4-Flag*}). After 24 h, the cells in each well were harvested and plated in 14 90-mm dishes and two 35-mm dishes. After 48 h, the media in each dish was replaced with 10 ml of culture medium (DMEM/10% FBS) supplemented with 10 mM HEPES (pH 7.2, Invitrogen), antibiotics, and 0.01 μM forskolin (Nacalai Tesque), and cultured at 30°C. After 12, 16, 20, 24, 28, 32, 36 h from the stimulation, the treated cells were fixed with 1% paraformaldehyde by a set of two dishes and used for Chromatin Immunoprecipitation. In the same time, bioluminescence was measured with photomultiplier tube (PMT) detector assemblies (LM2400, Hamamatsu Photonics) with the cells in 35-mm dishes, which was replaced with 2 ml of culture medium (DMEM/10% FBS) supplemented with 10 mM HEPES (pH 7.2, Invitrogen), 0.1 mM luciferin (Promega), antibiotics, and 0.01 μM forskolin (Nacalai Tesque). The modules and cultures were maintained in a darkroom at 30°C and interfaced with computers for continuous data acquisition. Photons were counted for 1 min at 12-min intervals.

Chromatin Immunoprecipitation assays with these NIH3T3 cells were performed as previously described[7] with the following modifications. In this report,

we used Chromatin Immunoprecipitation Assay Kits (Upstate Biotechnology), anti-FLAG M2 antibody (Sigma) and anti-V5 antibody (Sigma). Protein G-Sepharose (GE Healthcare) was used for precipitation of antibody/protein immune complexes. The resulting precipitated DNA was quantified by quantitative PCR. Quantitative PCR was performed using ABI Prism 7700 and Power SYBR Green Reagents (Applied Biosystems).Samples contained 1×Power SYBR Green Master Mix (Applied Biosystems), 0.5 μM primers and 1/25 ChIP product DNA in a 10 μl volume. The PCR conditions were as follows: 10 min at 95ºC, then 45 cycles of 15 s at 94ºC, 30 s at 59ºC and 1 min at 72ºC. Absolute DNA abundance was calculated using the standard curve obtained from NIH3T3 cell's genomic DNA and pG4-*dLuc* plasmid. The *Act* promoter (*Act*-5') and *Tbp* promoter (*Tbp*-5') regions were used as the internal control.

Primer sequence for Quantitative PCR of ChIP product.

UAS-forward: 5'-TAGGCTGTCCCCAGTGCAAG-3'

UAS-reverse: 5'-CGATAGAGAAATGTTCTGGCAC-3'

Act-5'-forward: 5'-CCAAGAGGCTCCCTCCACA-3'

Act-5'-reverse: 5'-GTGCAAGGGAGAAAGATGCC-3'

Tbp-5'-forward: 5'-GAGAGCATTGGACTCCCCAG-3'

Tbp-5'-reverse: 5'-AGCACCCACATGGCTACTCAC-3'

Quantitative PCR of *dLuc* mRNA. NIH3T3 cells were transfected on the same condition as ChIP assay (as described above), and harvested at same timing of ChIP assay. Total RNAs were purified from the harvested cells using TRIzol reagent (Invitrogen), and treated with DNaseI with RNeasy kit (QIAGEN) and RNase-free

DNase set (QIAGEN) according to the standard protocol. The cDNA was synthesized from 0.25 μg of total RNA with random 6mer (Promega) and Superscript II Reverse Transcriptase (Invitrogen) according to the standard protocol. Quantitative PCR was performed using ABI Prism 7700 and Power SYBR Green Reagents (Applied Biosystems). Samples contained 1×Power SYBR Green Master Mix (Applied Biosystems), 0.5 μM primers and 1/20 synthesized cDNA in a 10 μl volume. The PCR conditions were as follows: 10 min at 95ºC, then 45 cycles of 15 s at 94ºC, 30 s at 59ºC and 1 min at 72ºC. Absolute cDNA abundance was calculated using the standard curve obtained from NIH3T3 cell's genomic DNA and pG4-*dLuc* plasmid. *Gapdh* mRNA expression levels were quantified and used as the internal control.

Primer sequence for Quantitative PCR of mRNA.

Luciferase-forward: 5'-CTTACTGGGACGAAGACGAACAC-3'

Luciferase-reverse: 5'-GAGACTTCAGGCGGTCAACG -3'

Gapdh-forward: 5'-CAAGGAGTAAGAAACCCTGGACC-3'

Gapdh-reverse: 5'-CGAGTTGGGATAGGGCCTCT-3'

Peak-time estimation of transcription factors' binding and *Luciferase* mRNA.

First, we chose the largest points in the latter 4 time points (24 h - 36 h) for the dGAL4-VP16-FLAG ChIP and the *Luciferase* mRNA experiments, and the largest point in the former 4 time points (12 h - 24 h) for the dGAL4-FLAG ChIP experiment. Next, we fitted a quadratic function to 3 time points around the largest point for each experiment, and identified the top of the function as a peak-time of the experiment. The peak-times were converted into circadian time by using periods of simultaneously

measured Luciferase activities (21.66 for the *Luciferase* mRNA experiments, and 20.92 for the ChIP experiments), by the function: (the raw peak-time / the period of the *Luciferase* activity) * 24.

Construction of plasmid p3×CCE-TK-*dGal4-VP16* and p3×CCE-TK-*dGal4*. To construct activator or repressor plasmids regulated by thymidine kinase (TK) promoter, we modified the pCMV-*dGal4-VP16* or pCMV-*dGal4* vectors as follows. We amplified the TK promoter sequences from pMU2-P(TK) (unpublished, the origin of TK promoter was phRL-TK (Promega)) by PCR with a forward primer containing an *Bgl*II recognition sequence (5'-ATATATAGATCTCTAGCCCGGGCTCGAGATC-3') and a reverse primer containing a *Nhe*I recognition sequence (5'-GTAGTAGCTAGCCCGTTATAGTTACTGCAGAAGC-3'). The PCR product was then digested with *Bgl*II and *Nhe*I, and inserted in the pCMV-*dGal4-VP16* or pCMV-*dGal4* vectors, that were previously digested with *Bgl*II and *Nhe*I. To drive the artificial activator or repressor by CCE, the oligonucleotides containing three tandem repeat sequences of CCEs were annealed, and inserted into *Bgl*II site of the pTK-*dGal4-VP16* or pTK-*dGal4* vectors. The end products, p3×CCE-TK-*dGal4-VP16* and p3×CCE-TK-*dGal4* plasmids, were used as the activator or repressor plasmids for the artificial transcription circuits.

The oligonucleotide sequence for three tandem repeated clock-controlled element.

3× *Per2* E'-box-forward:

5'-GATCGCGCGCGCGGTCACGTTTTCCACTATGTGACAGCGGAGGGCGCGCG

CGGTCACGTTTTCCACTATGTGACAGCGGAGGGCGCGCGCGGTCACGTTTTC
CACTATGTGACAGCGGAG-3'

3× *Per2* E'-box-reverse:
5'-GATCCTCCGCTGTCACATAGTGGAAAACGTGACCGCGCGCGCCCTCCGCT
GTCACATAGTGGAAAACGTGACCGCGCGCGCCCTCCGCTGTCACATAGTGG
AAAACGTGACCGCGCGCGC-3'

3× *Per3* D-box-forward:
5'-GATCCCCGCGCGTTATGTAAGGTACTCGCCCGCGCGTTATGTAAGGTACT
CGCCCGCGCGTTATGTAAGGTACTCG-3'

3× *Per3* D-box-reverse:
5'-GATCCGAGTACCTTACATAACGCGCGGGCGAGTACCTTACATAACGCGCG
GGCGAGTACCTTACATAACGCGCGGG-3'

3× *Bmal1* RRE-forward:
5'-GATCAGGCAGAAAGTAGGTCAGGGACGAGGCAGAAAGTAGGTCAGGGA
CGAGGCAGAAAGTAGGTCAGGGACG-3'

3× *Bmal1* RRE-reverse:
5'-GATCCGTCCCTGACCTACTTTCTGCCTCGTCCCTGACCTACTTTCTGCCTC
GTCCCTGACCTACTTTCTGCCT-3'

Re-annotation of clock-controlled genes. The previously published genome-wide expression data for the liver [2] were re-analyzed and re-annotated to find transcription factors that showed circadian expression. Each probe set that was identified as a clock-controlled gene in the previous report [2], was annotated by using link information

in the Entrez Gene database (gene name, gene symbol, and Entrez Gene ID), link information in the TRANSFAC database (FACTOR, MATRIX, consensus binding sites, CLASS ID, and upstream transcription factors), the Affymetrix annotation file (InterPro ID), and information in the mammalian promoter/enhancer database (clock-controlled elements, E-box, D-box, and RRE) (Kumaki *et al.*, submitted). The annotation table is shown in **Supplementary Table 1** online.

Parameter search. First, the initial parameter set in the formulas of our theoretical model was randomly chosen except for K_A, K_R (=1/2), a (=0), b and n (=1). As multiplying by K_A, K_R is equivalent to dividing by both α_A, α_R and γ_A, γ_R , in the formula $T(t)$, K_A and K_R were fixed to a constant (1/2) to eliminate ambiguity. If the minimum amplitude of an output with a specific initial parameter set (obtained by changing the phase of the repressor) was too low or too high (<1/100 or >100-fold of a mean amplitude of an activator and a repressor), the initial parameter set was discarded and a new parameter set was randomly searched again.

Second, one parameter other than K_A, K_R, a, b, n was chosen, and then ten different values of the parameter were generated within 30-fold of its original value. For each value of the parameter, graphs like that in **Fig. 5a** and **b** were drawn by changing the value of b. The first graph (**Fig. 5a**) shows relationships between phase differences of the activator and the repressor (activator phase – repressor phase) and phase differences of the activator and the output protein (output protein phase – activator phase). The second graph (**Fig. 5b**) shows relationships between phase difference of the activator and the repressor and the relative amplitude of the output protein. The points in these graphs represent observed outputs of various combinations of activators and repressors. The parameter value that had the lowest

least squares distance to the measured experimental points was chosen as the new value of the parameter. We did not use *-marked points because these outlier points have larger (>4-fold amounts of the activator than the repressor) differences between amounts of the activator and the repressor (**Fig. 5c**), and also seem to have lower relative amplitudes. This second fitting procedure was repeated until no more improvements were observed, and the final parameter set was recorded as a fitted parameter set. By repeating these procedures, we found 100 fitted parameter sets.

Sensitivity analysis. All parameters except for *n* were analyzed for the degree to which the output phase and the relative amplitude was sensitive to them. To calculate the sensitivity of the output phase to a certain parameter, the value of the parameter was changed within 1 hour (0.5-hour advance and 0.5-h delay) for *a* or *b*, or changed within a 4-fold (one-half and double the original parameter value) if it was one of the other parameters. For each parameter change, the maximum changes in phase difference between the activator and the output were calculated for each *b* within $-12 < b < 12$, and the average value of the maximum phase change (or the change of the relative amplitude) was calculated over $-12 < b < 12$ and defined as the "phase change" (or "relative amplitude change") due to the parameter change. This procedure was performed for each parameter set in 100 fitted parameter sets. The average and SEM of the phase change due to the parameter change were then calculated over the 100 fitted parameter sets with trimming of the 5% outliers, and defined as the measures of sensitivity of the corresponding parameter change.

Construction of p3×E'-box-SV40-*Dbp* and p3×RRE-SV40-*E4bp4*. To construct *Dbp* and *E4bp4* gene expression vectors regulated by E'-box and RRE, the *Dbp* and

E4bp4 coding sequence were amplified from the pMU2-*Dbp* and pMU2-*E4bp4* plasmids (Kumaki *et al.*, submitted) by PCR with forward (5'-CTCGAAGGAGAGGCCACCATGGAC-3') and reverse (5'-GCACCCGACATAGATTCATTAACCC-3') primers, and phosphorylated by Mighty Cloning kit <Blunt End> (TaKaRa). The vectors for insertion of these PCR fragment were amplified from the p3×E'-box-SV40-*dGal4* and p3×RRE-SV40-*dGal4* plasmids (See **Methods** in main text) by invert PCR with forward (5'-GGTACCTGAATAACTAAGGCCGCTTCC-3') and reverse (5'-CAGGAGGCTTGCTTCAAGCTGGC-3') primers, and blunted by T4 DNA Polymerase, and then dephosphorylated by Bacterial Alkaline Phosphatase. The *dGal4* coding region was deleted by this treatment. The *Dbp* and p3×E'-box-SV40 PCR fragments, and *E4bp4* and p3×RRE-SV40 PCR fragments were ligated, respectively. These products were termed p3×E'-box-SV40-*Dbp* and p3×RRE-SV40-*E4bp4*, and used for perturbation experiment.

Perturbation experiments of natural transcriptional circuits to verify the predictions. Real-time circadian assays were performed as previously described[1,6] with the following modifications. NIH3T3 cells (American Type Culture Collection) were grown in DMEM (Invitrogen) supplemented with 10% FBS (JRH Biosciences) and antibiotics (25 U/ml penicillin, 25 mg/ml streptomycin; Invitrogen). Cells were plated at 1×10^5 cells per well in 35-mm dishes 24 h before transfection. These cells were transfected with FuGene6 (Roche) according to the manufacturer's instructions. The cells in each well were transfected with two plasmids (0.5 μg of p3×D-box-SV40-*dLuc*[1] reporter plasmid, 0, 0.1, 0.3, 0.6, 0.9, 1.2, 1.5 μg of p3×E'-box-SV40-*Dbp* or p3×RRE-SV40-*E4bp4*). The amount of transfected plasmid was adjusted to 2.0 μg with empty vector. After 72 h, the media in each well was

replaced with 2 ml of culture medium (DMEM/10% FBS) supplemented with 10 mM HEPES (pH 7.2, Invitrogen), 0.1 mM luciferin (Promega), antibiotics, and 0.01 μM forskolin (Nacalai Tesque). Bioluminescence was measured with photomultiplier tube (PMT) detector assemblies (LM2400, Hamamatsu Photonics). The modules and cultures were maintained in a darkroom at 30°C and interfaced with computers for continuous data acquisition. Photons were counted for 1 min at 12-min intervals.

References

1. Ueda, H.R. et al. System-level identification of transcriptional circuits underlying mammalian circadian clocks. *Nat Genet* **37**, 187-192 (2005).

2. Ueda, H.R. et al. A transcription factor response element for gene expression during circadian night. *Nature* **418**, 534-539 (2002).

3. Akhtar, R.A. et al. Circadian cycling of the mouse liver transcriptome, as revealed by cDNA microarray, is driven by the suprachiasmatic nucleus. *Curr Biol* **12**, 540-50 (2002).

4. Panda, S. et al. Coordinated transcription of key pathways in the mouse by the circadian clock. *Cell* **109**, 307-20 (2002).

5. Storch, K.F. et al. Extensive and divergent circadian gene expression in liver and heart. *Nature* **417**, 78-83 (2002).

6. Sato, T.K. et al. Feedback repression is required for mammalian circadian clock function. *Nat Genet* **38**, 312-319 (2006).

7. Yamashita, M. et al. Identification of a Conserved GATA3 Response Element Upstream Proximal from the Interleukin-13 Gene Locus. *J. Biol. Chem.* **277**, 42399-42408 (2002).